Linköping University | Department of Computer and Information Science
Bachelor's thesis, 16 ECTS | Electronics
202020 | LIU-IDA/LITH-EX-G--2020/Preliminary v0.9--SE

Reuse and verification of test equipment for ISO 7637

Återanvändning och verifiering av testutrustning för ISO 7637

Jonatan Gezelius

Supervisor : Peter Johansson
Examiner : Michael Josefsson

External supervisor : Gunnar Karlström

LINKÖPING UNIVERSITY

Linköpings universitet
SE–581 83 Linköping
+46 13 28 10 00 , www.liu.se

Abstract

Standards exist to unify requirements and to make it possible to make sure that equipment is tested in the same way, even if several different test labs performs the test. But as new technology comes to market, and old technology evolves, so must the standards. The International Organization for Standardization are continuously developing new standards and updating existing standards. And sometimes the specified tests changes, yielding old test equipment obsolete.

In this thesis, we will look at the differences between the old and the current versions of the ISO 7637 standards as well as how we can verify if old test equipment lives up to the new requirements. A verification method will be designed, partly implemented and evaluated. Several of the aspects for automating the verification will be considered. The results will show that old equipment most likely will be usable with the newer version of the standard, as well as point out some of the difficulties of verifyng that this is the case.

Acknowledgments

I would like to thank my supervisor Peter Johansson and examiner Michael Josefsson for their patience with me during this work, it has gone way past its deadline.

I would also like to thank Gunnar Karlström at BK Development AB for letting me do my thesis in their company, at which I ended up getting employed before I had time to finish it. I want to thank my other colleagues at work for their support, especially Jens Riedel for always reminding me and pushing me to finish my thesis.

Furthermore, I would like to thank Carl Einarsson and Filip Strömbäck for helping me out with technical details with LaTeXand for being good friends.

Finally, I would like to thank my two friends Filip Erkers Lindberg and Oskar Olsson for supporting me and bringing me to have fun once in a while during this long project.

Contents

List of Figures

List of Tables

1 Introduction

The standards ISO 7637, *Road vehicles – Electrical disturbances from conduction and coupling*, and ISO 16750, *Road vehicles – Environmental conditions and testing for electrical and electronic equipment*, are international standards that apply to equipment in road vehicles with a nominal supply voltage of 12 V or 24 V.

The standards states that the product shall withstand a sufficient amount of disturbances applied to its power supply. The reason for this beeing that there can be voltage surges and noise in a vehicle's power supply lines. In general, the source of disturbances and noise in a vehicle origins from inductance in other devices connected to the power line, the cables and the vehicles alternator in combination with switching of loads or the supply. [11, 9]

To test if a product comply with this standard, there is equipment that simulates different events on the power supply lines. The test events consists of voltage pulses that are applied to the DUT, device under test. The pulses of interest in this paper are denoted pulse 1, pulse 2a, pulse 3a, pulse 3b and load dump test A. The standard defines the different scenarios, raise and fall times of test pulses, repetition times etc. It also defines the functional requirements of the equipment during these tests for what is considered a passed or a failed test. [11, 9]

1.1 Motivation

The standard defines all the timing requirements that must be met, and also specifies the load conditions for which the requirements apply [11]. From time to time the standards are revised, which may alter the requirements form the previous versions of the standard. Test equipment might be constructed for the currently valid standards, and possibly older versions, but might not be compatible with newer versions. New equipment might not be affordable by smaller test labs, and can thus inhibit labs from performing tests for this standard.

An appealing alternative would be the possibility to reuse the test equipment that was used along with the older revision of the standard, as long as it is capable of performing the tests reliably. For this to be possible, the test equipment must be verified in some way so that it is possible to guarantee that the tests are performed according to the new standard.

1.2 Aim

The main goal of this work is to investigate the possibility of reusing test equipment, made for a previous version of a standard, with the current version of that standard and how to assure that the test results are reliable.

If the above goal is met, the verification process of the system is desired to be automated.

1.3 Research questions

The following questions will be answered in this paper:

1. Can test equipment made for ISO 7637-2:2004, be used for testing compliance against ISO 7637-2:2011, the newer version of the standard?
2. If it can; What considerations must be made to allow for automating the test and verification process?
3. If it can't; What causes the failure, and what possible fixes can be made to make the equipment usable for the newer standard?

1.4 Delimitations

This paper only compares the standard ISO 7637-2:2004 to ISO 7637-2:2011 and ISO 16750-2:2012, because these are the most recent versions of the standards.

This paper only considers Pulse 1, Pulse 2a, Pulse 3a, Pulse 3b and Load dump A. The main reason being that these are the pulses that the available equipment can generate, but also that these pulses share many properties and the method of analysing them will probably be very similar.

This paper only considers the test equipment for ISO 7637-2 that was available at the company, presented in Table 1.1, for the pratical tests.

Table 1.1: The test equipment available for the project

Brand	**Model**	**Description**
EMTEST	EFT 200A	Burst generator
EMTEST	MPG 200B	Micropulse generator
EMTEST	LD 200B	Load dump generator
EMTEST	CNA 200B	Coupling network

1.5 Report structure

The theory chapter presents all necessary theory to back up the methods used in the project.

The method chapter describes how the project was executed so that it can be replicated.

The result chapter is tightly coupled to the method chapter, in such a way that each header can be found in both. This allows for an easy correlation between the method and its result.

The discussion chapter reflects on the results achieved and comments on the methods used. This is also where source critisism is brought up.

The conclusion chapter reconnects the project to the original research questions. There are also some suggestions for topics that need further research related to the project.

2 Theory

This chapter introduces the theory and facts that are related to this project. It describes the necessary parts of the ISO standards, measurement theory and methods to analyse acquired data.

2.1 Previous research

No previous research directly relevant to the reuse of test equipment was found. Though research that has been made on topics relevant to project, such as measurement techniques and curve fitting, are presented in this theory chapter.

2.2 ISO standards

The ISO organisation, International Organization for Standardization, was founded in 1947 and has since published more than 22,500 International Standards. ISO standards does not only cover the electronic industry, but almost every industry. The purpose of the standards is to ensure safety, reliability and quality of products in a unified way, making international trade easier. The name ISO comes from the Greek word *isos*, which means *equal*. [2]

A standard is developed and maintained by a Technical Committee, TC. The TC consists of, amongst others, experts in the area that the standard concerns [7]. A new standard is only developed when there exists a need for this from the industry or other groups that may require it [3]. Existing standards are automatically scheduled for review five years after its last publication, but can manually be reviewed before that time by the committee [5]. During the review process it will be decided if the standard is still valid, need to be updated or if it should be removed [5].

The naming convention used for ISO standards is in the format *number-part:year*, where the *number* is the identifier to the unique ISO standard, *part* denotes the part of the standard if it is divided into several parts and *year* is the publishing year. For example; the name *ISO 7637-2:2011* refers to part 2 of the ISO 7637 standard published in 2011, whilst *ISO 7637-2:2004* would refer to an earlier version of the exact same document published in 2004.

To get hold of a copy of a standard, one need to buy it from ISO store or from a national ISO member. [6]

2.3 ISO 7637 and ISO 16750

The ISO 7637 standard, *Road vehicles — Electrical disturbances from conduction and coupling*, concerns the electrical environment in road vehicles. The standard consists of four parts, as of August 2019.

Part 1, *Definitions and general considerations*, defines some abbreviations and technical terms that are used throughout the standard. It also intended use of the standard. [10]

Part 2, *Electrical transient conduction along supply lines only*, defines the test procedures related to disturbances that are carried along the supply lines of a product. Both emission, disturbances created by the DUT, and immunity, the DUT's capability to withstand disturbances, are covered. This part defines the test pulses that are of interest for this project, and the verification of them. [11]

Part 3, *Electrical transient transmission by capacitive and inductive coupling via lines other than supply lines*, defines immunity tests against disturbances on other interfaces that the power supply. It focuses on test setups and different ways of coupling the signals. [12]

Part 5, *Enhanced definitions and verification methods for harmonization of pulse generators according to ISO 7637*, proposes an alternative verification method of the test pulses defined in ISO 7637-2. The main difference from the method described in ISO 7637-2 is that the DC voltage, U_A, should not only be 0 V during the verification, but also be set to the nominal voltage, U_N. This will not be considered deeply in this report, since it is only a proposal and makes the verification equipment more difficult. [13]

The ISO 16750, *Road vehicles – Environmental conditions and testing for electrical and electronic equipment*, concerns different environmental factors that a product might face in a vehicle, such as mechanical shocks, temperature changes and acids. Part 2 of the standard, *Electrical Loads*, deals with some electrical aspects that was previously part of the ISO 7637 standard. This is the only part of ISO 16750 that will be considered. [8, 9]

2.4 Test pulses

All test pulses defined in ISO 7637 and ISO 16750 are supposed to simulate events that can occur in a real vehicle's electrical environment, that equipment must be able to withstand. The properties of these test pulses are well defined, to allow for unified testing regardless of which test lab that performs the test. In the real world, however, the disturbances might of course differ from the test pulses since a real case environment is not controlled. [11, 9, 1]

The test pulses of interest defined in ISO 7637 are denoted *Test pulse 1*, *Test pulse 2a*, *Test pulse 3a* and *Test pulse 3b*. The test pulse of interest defined in ISO 16750 is denoted *Load dump Test A*. There are more pulses and tests defined in these standards, but those are not in the scope of this project.

The general characteristics in common for all pulses are the DC voltage U_A, the surge voltage U_s, the rise time t_r, the pulse duration t_d and the internal resistance R_i. The property *internal resistance* is only in series with the generated pulse, not in series with the DC power source. For pulses that are supposed to be applied several times, t_1 usually denotes the time between the start of two consecutive pulses. The timings are illustrated in Figure 2.1a.

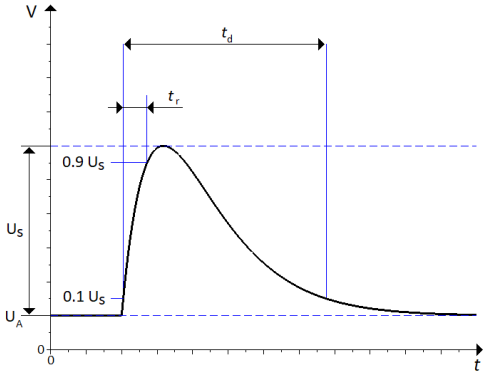

(a) The surge voltage U_S is the puse maximum voltage disregarding the offset voltage U_A. The rise t_r time is defined as the time elapsed from 0.1 to 0.9 times the surge voltage on the rising edge of the pulse. The duration t_d is defined as the time from 0.1 times the maximum voltage on the rising edge, back to the same level of the falling edge.

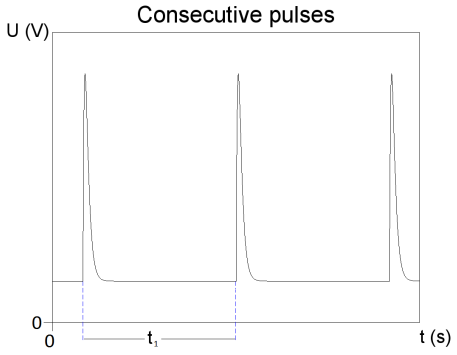

(b) The repetition time is defined as the time between two adjacent rising edges.

Figure 2.1: The common properties of the pulses, as defined by ISO 7637.

An important observation is that the definition of the surge voltage, U_s, differs in ISO 7637 and ISO 16750 as depicted in Figure 2.5.

Test pulse 1

This pulse simulates the event of the power supply being disconnected while the DUT is connected to other inductive loads. The other inductive loads will generate a voltage transient of reversed polarity onto the DUT's supply lines.

In the standard there are two additional timings associated to this pulse, t_2 and t_3, which are defining the disconnection time for the power supply during the voltage transient. In practice t_3 can be very short, specified to less than 100 µs, and the step seen in Figure 2.2 might be too short to be clearly distinguishable when seen on a oscilloscope.

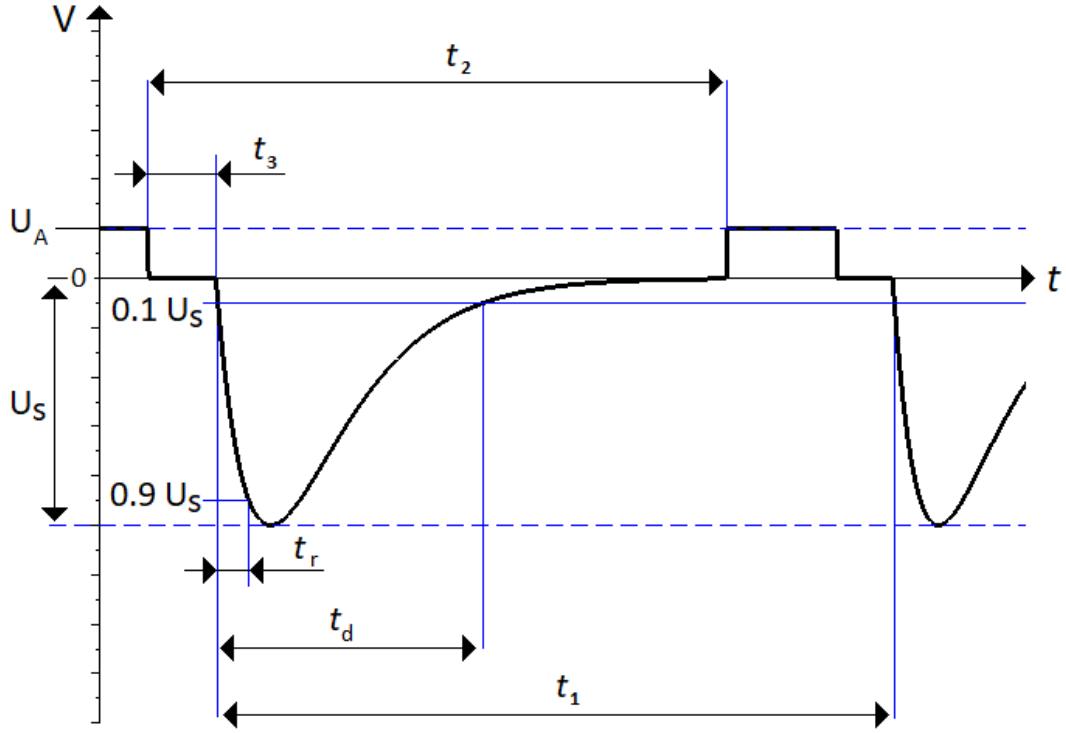

Figure 2.2: Illustration of test pulse 1.

Table 2.1: Parameter values for pulse 1

Parameter	12 V **system**	24 V **system**
U_A	13.8 V to 14.2 V	27.8 V to 28.2 V
U_S	−75 V to −150 V	−300 V to −600 V
R_i	10 Ω	50 Ω
t_d	2 ms	1 ms
t_r	0.5 µs to 1 µs	1.5 µs to 3 µs
t_1	≥0.5 s	
t_2	200 ms	
t_3	<100 µs	

Test pulse 2a

This pulse simulates the event of a load, parallel to the DUT, being disconnected. The inductance in the wiring harness will then generate a positive voltage transient on the DUT's supply lines. distinguishable when seen on a oscilloscope.

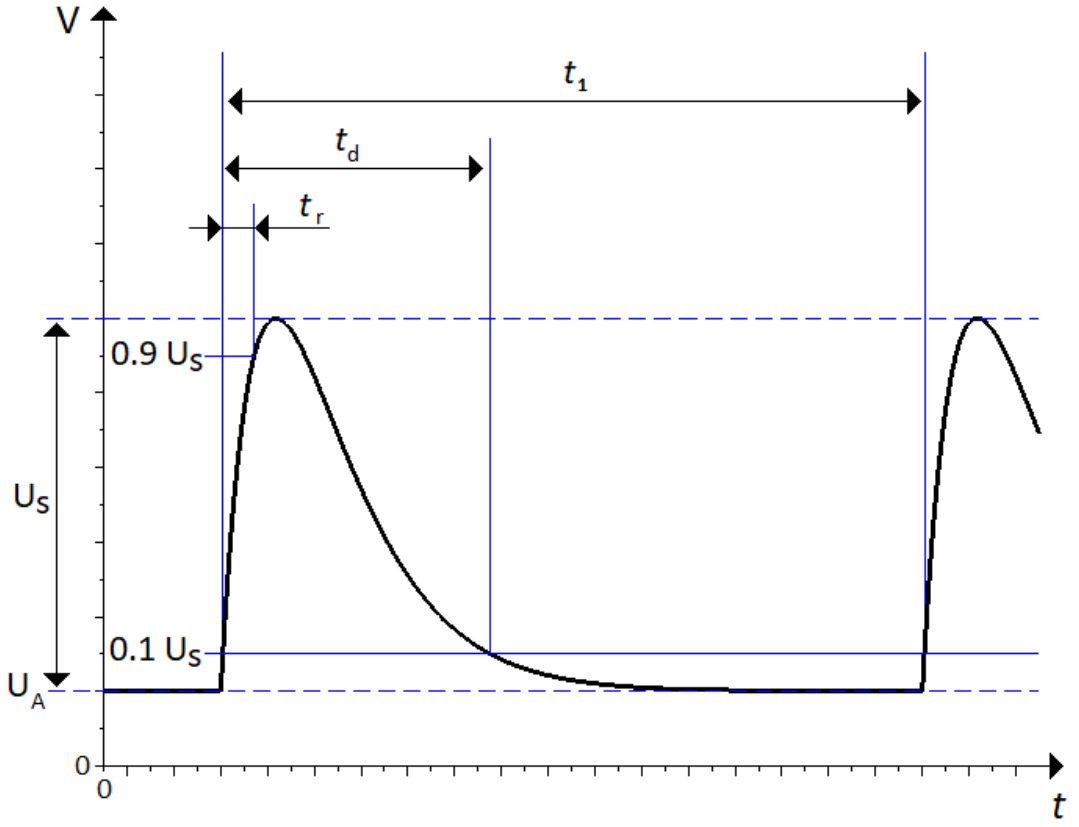

Figure 2.3: Illustration of test pulse 2a.

Table 2.2: Parameter values for pulse 2a

Parameter	12 V **system**	24 V **system**
U_A	13.8 V to 14.2 V	27.8 V to 28.2 V
U_S	37 V to 112 V	
R_i	2 Ω	
t_d	0.05 ms	
t_r	0.5 µs to 1 µs	
t_1	0.2 s to 5 s	

Test pulse 3a and 3b

Test pulse 3a and 3b simulates transients "which occur as a result of the switching process" as stated in the standard [11]. The formulation is not very clear, but is interperted and explained by Frazier and Alles [1] to be the result of a mechanical switch breaking an inductive load. These transients are very short, compared to the other pulses, and the repetition time is very short. The pulses are sent in bursts, grouping a number of pulses together and separating groups by a fixed time.

These pulses contain high frequency components, up to 100 MHz, and special care must be taken when running tests with them as well as when verifying them.

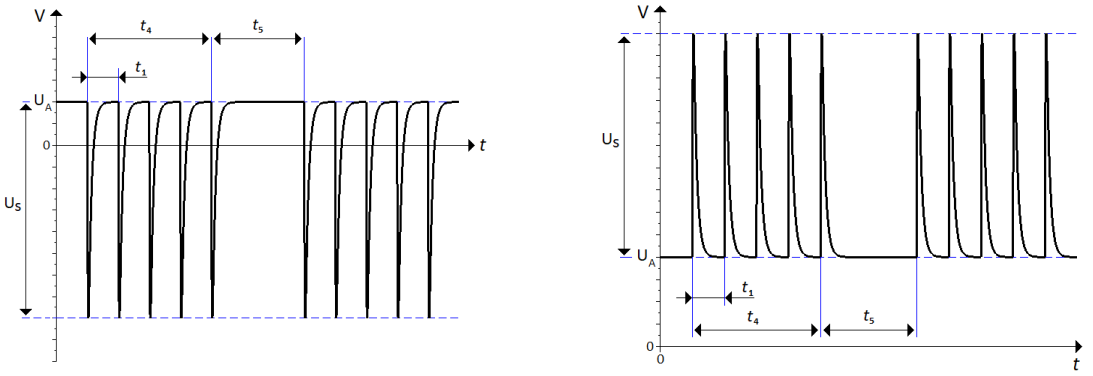

(a) Pulse 3a

(b) Pulse 3b

Figure 2.4: Pulse 3a and 3b are applied in bursts. Each individual pulse is a double exponential curve with the same properties, t_r and t_d, as e.g. pulse 2a

Table 2.3: Parameter values for pulse 3a and 3b

Parameter	12 V **system**	24 V **system**
U_A	13.8 V to 14.2 V	27.8 V to 28.2 V
Pulse 3a U_S	−112 V to −220 V	−150 V to −300 V
Pulse 3b U_S	75 V to 150 V	150 V to 300 V
R_i	50 Ω	
t_d	105 ns to 195 ns	
t_r	3.5 ns to 6.5 ns	
t_1	100 µs	
t_4	10 ms	
t_5	90 ms	

Load dump Test A

The Load dump Test A simulates the event of disconnecting a battery that is charged by the vehicles alternator, the current that the alternator is driving will give rise to a long voltage transient.

This pulse has the longest duration, t_d, of all the test pulses. It also has the lowest internal resistance. These properties makes it capable of transferring high energies into a low impedance DUT or dummy load.

Prior to 2011, the Load dump Test A was part of the ISO 7637-2 standard under the name *Test pulse 5a*. The surge voltage U_s was in the older standard, ISO 7637-2:2004, defined as the voltage between the DC offset voltage U_A and the maximum voltage. In the newer standard, ISO 16750-2:2012, U_s is defined as the absolute peak voltage. Only the former definition is used in this paper, $U_s = \hat{U} - U_A$.

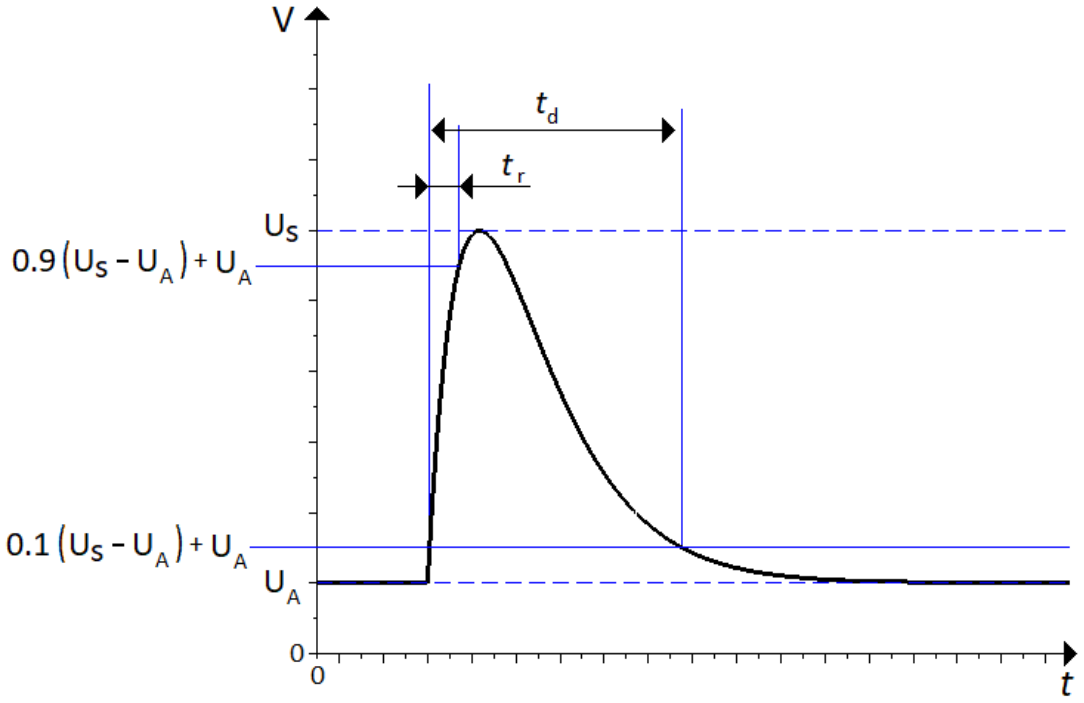

Figure 2.5: Illustration of load dump Test A. Note the different definition of U_S compared to the other pulses.

Table 2.4: Parameter values for load dump Test A

Parameter	12 V **system**	24 V **system**
U_A	13.8 V to 14.2 V	27.8 V to 28.2 V
U_S ISO 16750	79 V to 101 V	151 V to 202 V
U_S ISO 7637	64.8 V to 87.2 V	122.8 V to 174.2 V
R_i	0.5 Ω to 4 Ω	1 Ω to 8 Ω
t_d	40 ms to 400 ms	100 ms to 350 ms
t_r	5 ms to 10 ms	

Application of test pulses

During a test, the nominal voltage is first applied between the plus and minus terminal of the DUT's power supply input by the test equipment. Then a series of test pulses are applied between the same terminals. The pulses are repeated at specified intervals, t_1, as depicted in Figure 2.1b.

An example of how a test pulse can be applied by the test equipment is depicted in Figure 2.6.

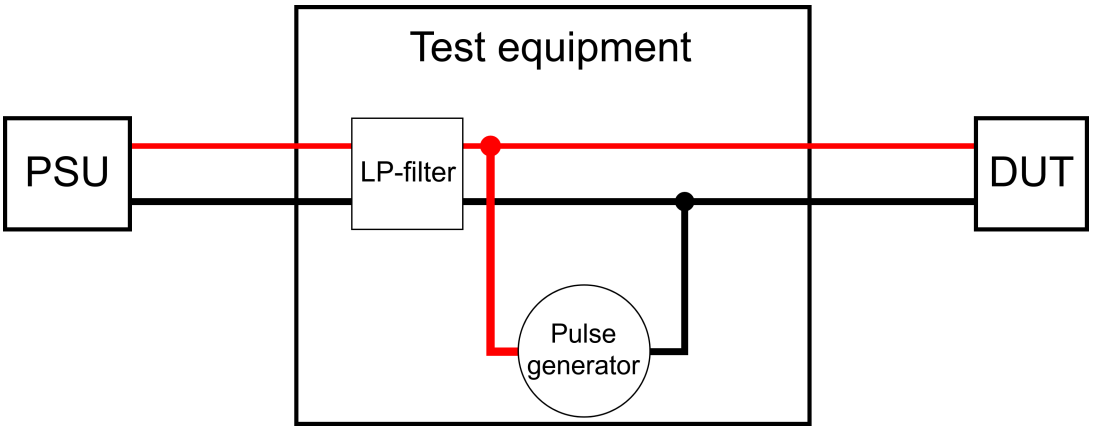

Figure 2.6: Illustration of how the test equipment can apply a test pulse to the DUT whilst also providing the DC supply throuht an external PSU.

Verification

The test pulses are to be verified before they are applied to the DUT. The voltage levels and the timings are to be measured both without any load, and with a matched load, $R_L = R_i$, attached. The standard omits the rise time constraint when the load is attached, except for pulse 3a and 3b. [11]

The verification is to be conducted with U_A set to 0. There is, however, a proposal to set U_A equal to the nominal voltage during the verification process, as the behaviour of the pulse generators has proven differ in this case [13]. In this project $U_A = 0$ will be used.

The limits, and tolerances, for the pulses are summarised in Table 2.5. The matched loads are to be within 1% of the nominal value.

The instruments used for measuring the pulses must have at least 400 MHz, since pulse 3a and 3b contains frequency components of up to 200 MHz.

Table 2.5: These are all of the verifications that needs to be made before each use of the equipment, along with the limits for each case.

		Limits		
Pulse	Match resistor	U_S	t_d	t_r
Pulse 1, 12 V, Open		−110 V to −90 V	1.6 ms to 2.4 ms	0.5 µs to 1 µs
Pulse 1, 12 V, Matched	10 Ω	−110 V to −90 V	1.6 ms to 2.4 ms	0.5 µs to 1 µs
Pulse 1, 24 V, Open		−660 V to −540 V	0.8 ms to 1.2 ms	1.5 µs to 3 µs
Pulse 1, 24 V, Matched	50 Ω	−660 V to −540 V	0.8 ms to 1.2 ms	1.5 µs to 3 µs
Pulse 2a, Open		67.5 V to 82.5 V	40 µs to 60 µs	0.5 µs to 1 µs
Pulse 2a, Matched	2 Ω	67.5 V to 82.5 V	40 µs to 60 µs	0.5 µs to 1 µs
Pulse 3a, Open (1k)		−220 V to −180 V	105 ns to 195 ns	3.5 ns to 6.5 ns
Pulse 3a, Match	50 Ω	−120 V to −80 V	105 ns to 195 ns	3.5 ns to 6.5 ns
Pulse 3b, Open (1k)		180 V to 220 V	105 ns to 195 ns	3.5 ns to 6.5 ns
Pulse 3b, Match	50 Ω	80 V to 120 V	105 ns to 195 ns	3.5 ns to 6.5 ns
Load dump A, 12 V, Open		90 V to 110 V	320 ms to 480 ms	5 ms to 10 ms
Load dump A, 12 V, Matched	2 Ω	90 V to 110 V	320 ms to 480 ms	5 ms to 10 ms
Load dump A, 24 V, Open		180 V to 220 V	280 ms to 420 ms	5 ms to 10 ms
Load dump A, 24 V, Matched	2 Ω	180 V to 220 V	280 ms to 420 ms	5 ms to 10 ms

2.5 Resistors at high frequencies

When working with resistors at high frequencies, one must consider the parasitc properties of the resistor. Vishay presents a model which consists of the resistance R, internal inductance L, internal capacitance C, external lead inductance L_C and external ground capacitance C_G.

Since the external ground capacitance is very small in comparison to the other parasitics, it has been neglected in this thesis. The model used for the simulations is depicted in Figure 2.7, with the values L = 0.1 nH, C = 1 pF and L_C = 1 nH. This is a bit higher than the values in Vishays paper, but those are also for smaller packages. [16] An approximation of the combined inductance of more than 1 nH for the 1206 package is also in line with the values in a technical information note from AVX for capacitors, the package lead inductance should be similar for capacitors and resistors[14].

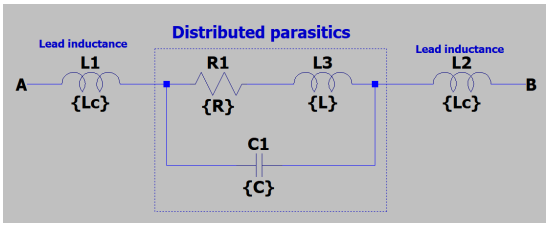

Figure 2.7: At high frequencies a resistors parasitic inductance and capacitance will affect the behavior of the circuit. This is the model used in this thesis when simulating circuits.

2.6 Measurement

There are several measurement methods needed during the project. To verify the test pulses, voltage has to be measured over time. To verify the dummy loads, resistance has to be measured. To verify the attenuators, their magnitude response has to be measured. This chapter describes the necessary measurement theory required for this project.

Resistance

To measure resistance, a current is fed through the resistor and the resulting voltage is measured to calculate the resistance using ohms law. This is typically carried out using a multimeter and two probe wires connecting to each terminal of the resistor. When measuring very low valued resistors, however, the resistance in the probe wires can be significant in relation to the resistor measured and will affect the accuracy. One way of overcoming this is to perform a 4-wire measurement using a so called *Kelvin connection*. In this method the current that is fed through the resistor using one pair of wire, and the resulting voltage is measured at the desired point using another pair according to Figure 2.8.[17]

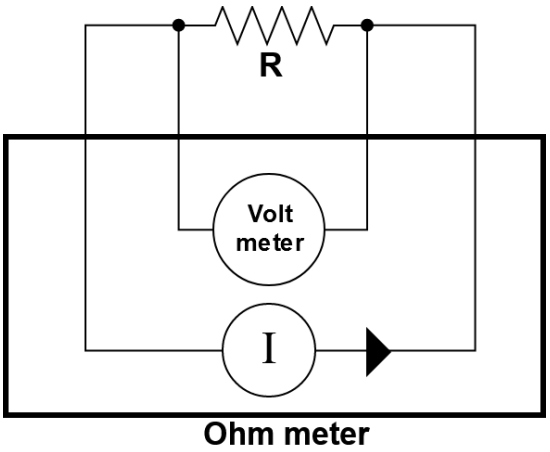

Figure 2.8: When measuring a low value resistor, the *Kelvin connection* can be used to determine the resistance at the point where the voltmeter is connected without the resistance in the probe leads affecting the result.

Oscilloscopes, bandwidth, rise time and probes

When using an oscilloscope to measure voltage over time, there are several limiting factors to how fast signals one can measure. The oscilloscope itself has a specified bandwidth, as do the probe and any attenuators used. All of these combined determine how short rise times that can be measured accurately. The rise time of the measured will be affected by these properties and the rise time displayed on the oscilloscope screen will be approximately according to Equation 2.1, where T_N is the 10 % to 90 % rise time limit for each part in the chain. [15]

$$T_{rise\ composite} = \sqrt{T_1^2 + T_2^2 + ... + T_N^2} \tag{2.1}$$

Since Equation 2.1 is based on the rise time limitation but the specification usually tells the 3 dB bandwidth, a conversion can be made according to Equation 2.2. [15]

$$T_{10-90} = \frac{0.338}{F_{3\,\mathrm{dB}}} \tag{2.2}$$

2.7 Analysis

The data points from the measurement must be processed and evaluated to determine if the measured pulse is within the specified limits.

Mathematical description

All of the test pulses applied to the vehicle equipment can individually be described mathematically by variations of the double exponential function shown in Equation 2.3. The properties of interest, the ones which are specified in the standards, are the surge voltage U_s, the rise time t_r, the duration t_d and the repetition time t_1. [11]

$$u(t) = k(e^{\alpha t} - e^{\beta t}) + U_A \tag{2.3}$$

It is not in the scope of this report to actually fit this function to the measured pulse, and further analyze it.

2.8 Instrumentation and control

The following chapter describes the different instruments that were used, and their control interfaces.

Tektronix TDS7104 Oscilloscope

The oscilloscope available for this project is a Tektronix TDS7104, with specifications as seen in Table 2.6. It has GPIB interface and TekVISA GPIB, an API for sending GPIB commands over ethernet, available for remote control. [1]

Table 2.6: Specs of the Tektronix TDS7104

Bandwidth	1 GHz
Sample rate	10 GS/s
Channels	4
Interfaces	GPIB, TekVISA

xxxxx Isolated differential probe

TODO

TODO:
Peta in kort beskrivning av prob och dess data

EM Test MPG 200 Micropulse generator

The MPG 200 is used to generate *Test pulse 1* and *2a*. MPG is an abbreviation for *MicroPulse Generator*. The instrument is designed to generate test pulses according to the older ISO 7637-2:1990 version, but the parameters can be adjusted to comply with the new ISO 7637:1990 standard. The adjustable parameter ranges are shown in Table 2.7. The instrumentation panels can be seen in Figure 2.9.

Table 2.7: Adjustable parameters in the MPG 200

Parameter	Range
U_S	20 V to 600 V
U_S polarity	+, -
R_s	2 Ω, 4 Ω, 10 Ω, 20 Ω, 30 Ω and 50 Ω
t_1	0.2 s to 99.0 s
t_2	0 s to 10 s

EM Test EFT 200 Burst generator

The EFT 200 is used to generate *Test pulse 3a* and *3b*. EFT is an abbreviation for *Electrical Fast Transient*. The instrument is designed to generate test pulses according to the older ISO 7637-2:1990 version, but the parameters can be adjusted to comply with the new ISO 7637:1990 standard. The adjustable parameter ranges are shown in Table 2.8. The instrumentation panels can be seen in Figure 2.10.

[1] `https://www.tek.com/datasheet/tds7000-series`

(a) Front.

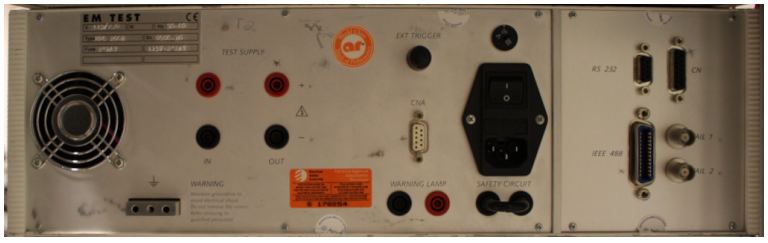

(b) Back.

Figure 2.9: The MPG 200 is used to generate test pulse 1 and 2a.

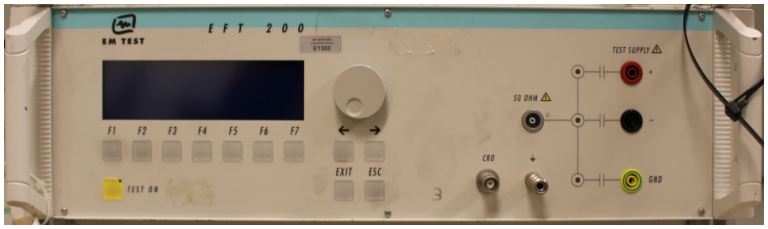

(a) Front.

(b) Back.

Figure 2.10: The EFT 200 is used to generate test pulse 3a and 3b.

Table 2.8: Adjustable parameters in the EFT 200

Parameter	Range
U_S	25 V to 1500 V
U_S polarity	+, -
Coupling	any combination of +, - and GND

EM Test LD 200 Load dump

The LD 200 is used to generate *Load dump Test A*. LD is an abbreviation for *Load Dump*. The instrument is designed to generate test pulses according to the older ISO 7637-2:1990 version, but the parameters can be adjusted to comply with the new ISO 16750:2012 standard. The adjustable parameter ranges are shown in Table 2.9. The instrumentation panels can be seen in Figure 2.11.

(a) Front.

(b) Back.

Figure 2.11: The LD 200 is used to generate load dump test a.

Table 2.9: Adjustable parameters in the LD 200

Parameter	Range
U_S	20 V to 200 V
R_s	0.5 Ω, 1 Ω, 2 Ω and 10 Ω
t_d	50 ms to 400 ms

EM Test CNA 200 Coupling Network

The SNA 200 is a coupling network used to multiplex the pulse generators outputs. It contains several relays to select the appropriate generator output. The SNA 200 has one interface for each pulse generator, but no interface for a computer. It is automatically controlled by the pulse generators. This allows the DUT to be connected only to the CNA 200 and not to each individual pulse generator. Figure 2.12 shows the connections between the instruments in this setup. There is also a coaxial connection for calibration of pulse 3a and pulse 3b on the front panel. The instrumentation panels can be seen in Figure 2.13.

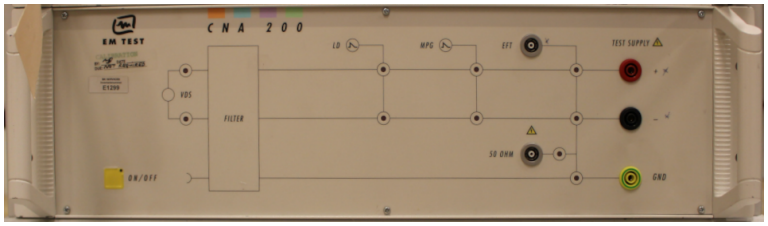

(a) Front.

(b) Back.

Figure 2.13: The CNA 200 is used to couple all of the other pulse generators outputs to a common output.

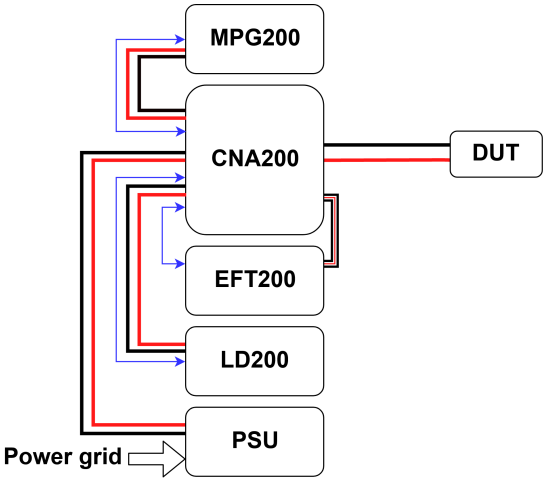

Figure 2.12: The CNA 200 allows each pusle generator to output their pulses through a common interface towards the DUT.

Rohde & Schwarz ZVL13

The ZVL13 is a vector network analyzer that operates in the frequency range 9 kHz to 13.6 GHz. It is, in this project, used to measure the magnitude and phase response between its two ports.

PAT 50 and PAT 1000

These are two attenuators that are made for verification of other burst test equipment, according to EN 61000-4-4. But their specifications, seen in Table 2.10, are suitable for this project. The attenuators can be seen in Figure 2.14.

Table 2.10: Specs of the PAT attenuators

Property	PAT 50	PAT 1000
Max voltage	8 kV	
Nominal attenuation	54 dB	60 dB
Input impedance	50 Ω ± 2 %	1000 Ω ± 2 %
Output impedance	50 Ω ± 2 %	
Bandwidth	400 MHz	

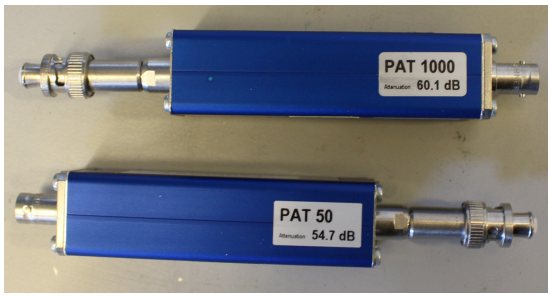

Figure 2.14: The two attenuators that were used in the project.

3 Methods

This chapter covers the methodologies used during the project.

3.1 Prestudy

During the project efforts were made to find relevant research using Linköping University Library's[1] and Google Scholar's[2] search engines.

Since the equipment intended for this project was untested before the project start, the first step was to hook it up and make some initial measurements to be able to decide the continuation of the project.

If the equipment seem to be mostly in line with the new standard requirements, the project plan was to go along the following path:

1. Investigate test architectures suitable for automatic testing and verification.
2. Design any utilities needed for the test and verification setup.
3. Implement the test architecture and any necessary utilities.
4. Measure and evaluate the system and the utilities.

If the equipment proved to deviate to much from the standard requirement, the project should go along the following path:

1. Investigate possible causes and fixes for the failure.
2. Design any utilities needed for the equipment to pass.
3. Implement these utilities.
4. Measure and evaluate the system with these utilities manually.

In either case, the following tasks should be considered if there is time:

[1] `https://liu.se/en/library`
[2] `https://scholar.google.se/`

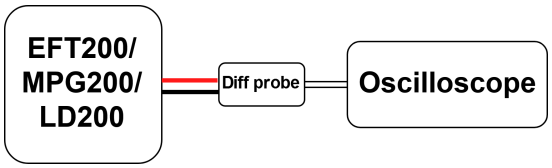

(a) Without CNA.

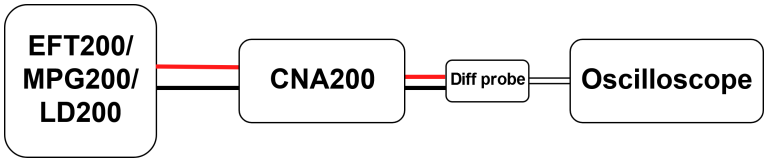

(b) With CNA.

Figure 3.1: The setup for measuring for pulse 1, pulse 2a and Load dump A.

1. Investigate possible methods, or algorithms, that can automatically verify the pulse shapes and parameters.
2. Implement a number of these methods.
3. Evaluate these methods.

3.2 Comparison between the old and the new standard

Since the equipment used in the project is designed for the older version of the standard, ISO 7637-2:2004 and possibly even ISO 7637-1:1990 together with ISO 7637-2:1990, the differences will be examined. This is done simply by comparing the standards side by side and noting the differences.

3.3 Examination and initial measurement of the old equipment

To decide the forthcoming of the project, the equipment first had to be checked to see if it is capable to operate within the limits for use with the newer standard. Because there is no dummy loads available at this point of the project, only open load measurements could be done.

With exception for Pulse 3a and Pulse 3b, all of the pulses were measured with the use of the high voltage differential probe described in section 2.8. The pulses are measured both directly on each generator connected according to Figure 3.1a and also through the coupling network CNA 200, as depicted in Figure 3.1b.

Pulse 3a and Pulse 3b was measured using the attenuators described in section 2.8 connected directly to the coaxial connector according to Figure 3.2a without the CNA. They were also measured connected through the CNA, directly to the coaxial connector according to Figure 3.2b. Thanks to the 50-ohm attenuator, PAT-50, this pulse could be measured in its matched state. The measurement in open state is a compromise, since a passive attenuator that does not load the input would be impossible to make, and was made as a 1000-ohm attenuator instead.

3.4 Test architecture

The total number of tests needed to verify the testing equipment before each product test is 14, according to Table 2.5. There are in total three different values for dummy loads. In practice these could be represented by two high frequency attenuators for pulse 3a and pulse 3b, since

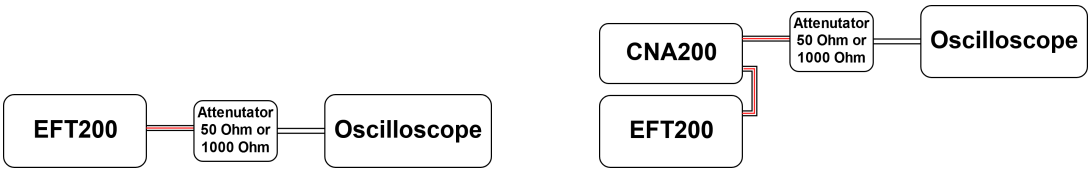

(a) Without CNA. (b) With CNA.

Figure 3.2: The setup for measuring for pulse 3a and pulse 3b.

these have really short rise times that will be affected much by parasitics of components, and three different high power dummy loads for the slower pulses where the parasitic effects might be negligible but the withstand power must be higher.

The following test architectures were considered, together with the external supervisor at the company.

Additionally there needs to be some sort of measurement fixture for evaluating the verification equipment.

Alternative 1 – Human assisted

The test can be performed semi-automatically by means of the existing equipment complemented by some dummy loads and, in the same manner the manual performance tests were executed. A computer could control the equipment and compare the results, by the assist of a human that can make the necessary reconnections between the tests. A proposed setup for this is shown in Figure 3.3.

The main advantage of this alternative is that it would require the least amount of hardware development time. It also doesn't need any extra hardware except from the dummy loads needed to do the verification.

The biggest disadvantage is that it would be very cumbersome to perform and also prone to human error. If the verification list is studied carefully one can minimize it to five reconnections after the initial connections are made, for example in the following order: No load, 2 Ω, 10 Ω, 50 Ω low frequency, 50 Ω high frequency, 1 kΩ high frequency.

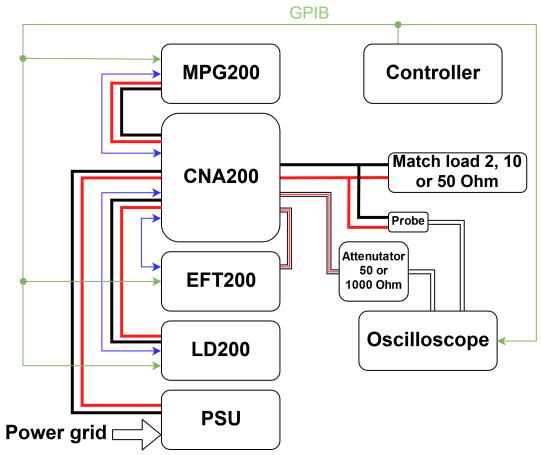

Figure 3.3: The proposed setup for alternative must be connected in different ways by a human during the verification process.

Alternative 2 – Fully automatic rig with external attenuators

To accurately measure Pulse 3a and Pulse 3b, the probes should be attached as close as possible to the generator because of the high frequency, to avoid influence of the connecting wires. This

could be accomplished by the means of a fixture that is attached directly to the generator, which can switch the pulses to the different loads or to the measurement outputs.

The dummy loads for all pulses, but Pulse 3a and Pulse 3b, will need to be put in a separate enclosure because of the high power dissipation. The proposed dummy loads for pulse 3a and pulse 3b is the external attenuators PAT 50 and PAT 1000. A proposed setup is depicted in Figure 3.4.

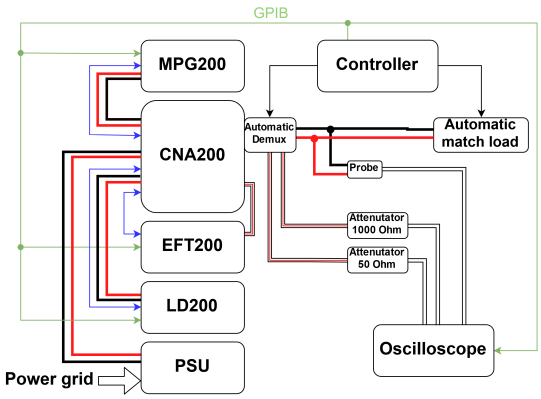

Figure 3.4: The proposed setup for alternative 2 is fully automatic, but exposes high voltage connectors between the demultiplexer and the two attenuators, marked with a red line.

The advantage of this method is that the verification can be performed fully automatically, except for the initial connection of the test rig. This also uses the commercially created attenuators that are already available.

The disadvantage to this setup is that the fixture needs to be designed, making the development costs greater. The fixture that attaches to the generator will expose high voltage on its measurement connectors, making it a safety hazard.

Alternative 3 – Fully automatic rig with embedded attenuators

To cope with the high voltage exposure, of alternative 1, the high frequency attenuators can be embedded inside the switching fixture, removing the need for high-voltage connectors. Figure 3.5.

To design Alternative 3 some utilities needs to be designed, namely:

- Relay box, the fixture with embedded attenuators that are to be attached to the front of the CNA.
- Match box, the dummy loads with some relays to be able to switch between them.

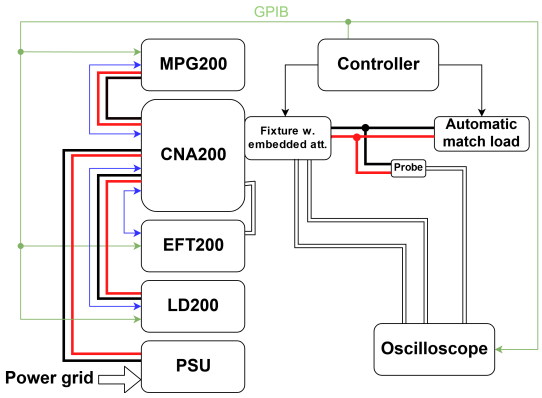

Figure 3.5: The proposed setup for alternative 3 have no high voltage connectors exposed during the calibration.

The advantages of this, in addition to the advantages of alternative 2, are that there is no longer need for external attenuators and that the connectors will no longer expose high voltage.

The disadvantage of this would be that the embedded attenuators might prove difficult to design. They need to be accurate up to high frequencies, be tolerable to high voltage, dissipate the power necessary and also be electrically safe.

3.5 Design of dummy loads

Each dummy load must withstand the applied test pulses, and preferably the worst possible test pulse for the specific dummy load even though it might not be intended. The dummy loads must have a tolerance of 1 % or less and be non-inductive. [11]

The dummy loads consists of one or more resistors. When determining whether the resistors withstands the test pulses, the parameters of interest are power dissipation, maximum voltage and maximum energy applied over time.

Since the pulse generators in most cases can generate a higher voltage than required by the standard, the dummy loads should be designed for the worst case setting on the generator. This mitigates the risk of overloading the dummy load caused human error or an error in the control system.

Three different dummy loads are needed. One 2 Ω load for load dump A and for pulse 2a, one 10 Ω load for pulse 1 in 24 V systems and one 50 Ω load for pulse 1 in 24 V systems.

Components

At first the momentary worst case powers and voltages were calculated by hand, using Equation 3.1. But to find components that withstand these high momentary powers proved very difficult, and it is not necessary since the pulse power is only high for a very short time.

$$P_{peak} = \left(\frac{U_S}{R_S + R_L}\right)^2 R_L \tag{3.1}$$

Instead of selecting components based on peak power they can be selected based on energy over time. Although, not all manufacturers specify this data in the datasheet. To get the proper values for this project, a simulation was made with LTSpice. The simulated circuit can be seen in Figure 3.6. There are preconstructed models for all of the relevant pulses, but the parameters are not tweakable. Thus, the pulse offset is removed, the magnitude is normalized and then multiplied by the desired U_S using the behavioural voltage source. The

power dissipated in the dummy load is then integrated over time to achieve the energy. The simulated circuit translates to the calculation shown in Equation 3.2.

$$E_{dummyload} = \int_{t_0}^{t_1} P(t)dt \tag{3.2}$$

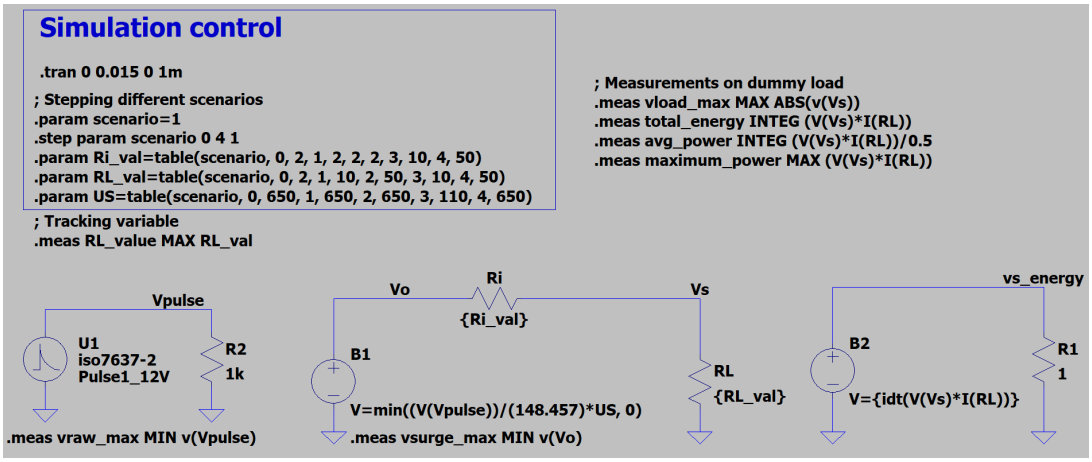

Figure 3.6: The energy transferred to the dummy load was simulated using the above LTSpice circuit for pulse 1. Similar circuits was used for the other pulses.

Based on the energy in each load, the minimum number of resistances could be achieved by dividing the energy from simulation by the energy specified in the resistor's datasheet.

PCB

Since most of the test pulses exceedes the properties of most resistors available, the dummy loads will be constructed of many resistors to share the power. It was decided to design a circuit board to connect all the discrete resistors. Not only does a PCB ease the connectivity of many components, it also gives good mechanical control of the resistors and the possibility to design for good heat dissipation.

Both the circuit schematic and layout editing of the board were performed in the free EDA, Electronic Design Automation, tool KiCad[1].

Before ordering the PCB, it was printed in 1:1 scale and attached to a piece of card board. The card board was then populated with the components already at hand to ensure that the footprints are correct and that the placement of the components makes sense and does not collide.

Measurements

When the dummy loads had been assembled, their resistances were determined using four wire resistance measurement directly at the PCB's connection points, as described in section 2.6.

3.6 Design of the switching fixture and the embedded attenuators

The chosen implementation requires a fixture with switches and attenuators, which purpose is to multiplex the pulse to the desired attenuator or to the dummy load. The principle is shown in Figure 3.7.

[1]KiCad EDA `http://kicad-pcb.org/`

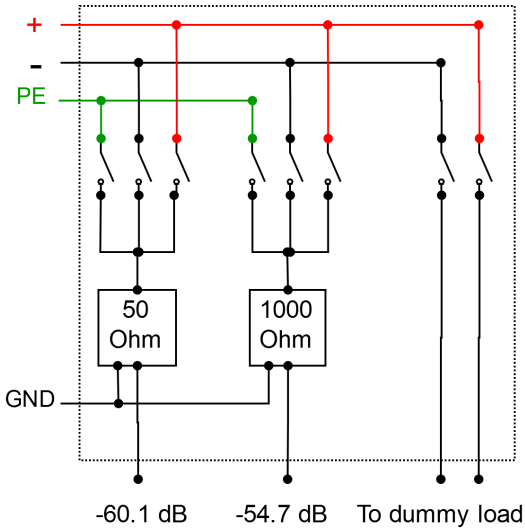

Figure 3.7: The multiplexing relay box can couple each of the three inputs through any of the attenuators. It can also connect the external dummy load to the + and - signal.

Only Pulse 3a and Pulse 3b were considered when designing these attenuators, since all other test pulses will be coupled to the separate dummy load. The attenuators must be able to withstand the pulse energies and voltages and should not distort the pulses. Preferably, the attenuators should also be able to withstand the worst case settings in the pulse generator with regard to voltage and power.

Components

The same methods were used for the attenuators as for the dummy loads to determine the number of resistors needed to share the power and voltage.

The relays were chosen based on high breakdown voltage between open contacts.

Attenuators

The target attenuation was decided to mimic the commercial attenuators, introduced in section 2.8, where the 50 Ω attenuator has an attenuation of 54.7 dB and the 1000 Ω attenuator has an attenuation of 60.1 dB.

The two attenuators were implemented as Π-attenuators. The values for the attenuators were retrieved from an online calculator[1], and then simulated in LTSpice to verify the values.

By dividing the attenuators into two Π-networks, the series resistance required is lower compared to realizing them in a single Π-link. This is desirable because the parasitic capacitance, which is dependent of the resistor package and not the resistance value, will influence a high value resistor at lower frequencies than it would on a low value resistor, as explained in section 2.5.

When the ideal resistor values had been achieved, the power over time and maximum voltage for each resistor was retrieved by simulation in a similar way as for the dummy load described in section 3.5. Based on this, the minimum number of discrete resistors needed to withstand the pulse energy was calculated. The minimum number of series resistors to withstand the maximum pulse voltage was also retrived from the simulation.

[1] Π attenuator calculator `https://chemandy.com/calculators/matching-pi-attenuator-calculator.htm`

With the minimum number of discrete resistors needed for each ideal resistor known, a constellation of available resistor values was constructed to approximate the nominal value with as few resistors as possible.

When the number of resistors and their constellations was decided, all of the discrete ideal resistors were replaced with non-ideal models in the simulation software. Each lead inductance was set to 1 nH, the internal inductance was set to 0.1 nH and the internal capacitance was set to 1 pF. Then the attenuators were checked in frequency domain, as well as how the pulses were affected in time domain. If the required 400 MHz bandwidth could not be achieved, frequency compensation with capacitors was attempted.

PCB

A PCB was designed for the attenuators and the switches. This gives good control of the lengths of the conductors, which is of importance when designing for higher frequencies. It is also possible to use the PCB for other mechanical purposes. For example to fit connectors in a desired constellation.

The design process followed the same methods as for the dummy load PCB. But because of the higher voltages some special considerations had to be made.

The measurement connectors accessible on the outside of the encapsulation must safe at all times. This involves keeping a minimum creepage distance of 6 mm to any trace that carry a high voltage, according to the regulations in EN 60664-1 [4].

The EDA tool has functionality for design rule checking, DRC, but there are some limitations in this function that inhibit its use in this case. The DRC in KiCad only allows to set the clearance for a specified net to all other nets. In this case it is only desired to restrict the clearance between the high voltage traces to the traces that must be considered safe. It is allowed for one high voltage trace to be close to another high voltage trace, it is only the functional isolation requirement of 3 mm that applies here. The output signal and the output ground can also be close to each other, since both are considered safe.

The high voltage traces were placed on the top layer of the PCB, while all signal traces were placed on the bottom layer. To aid the design process without the DRC, a workaround was used to ensure that that enough clearance was kept between the pads and the traces. The 6 mm clearance was added to the package footprint as a graphical circle on a user layer in the EDA, as seen in Figure 3.8. This is not an enforced rule, but it helps during the manual design process.

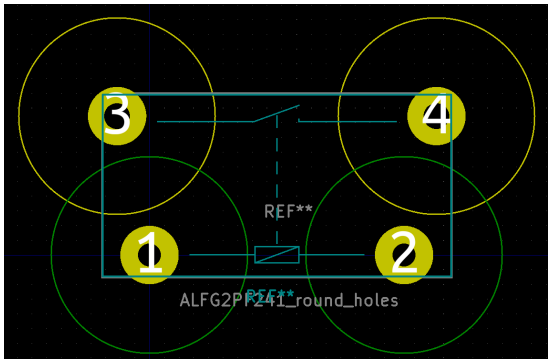

Figure 3.8: Decorational circles were made on the relay footprint to mark the creepage and clearance distance required.

The layout was printed in 1:1 scale to verify the layout in the same way as for the dummy load. This was especially important due to the critical positioning of the 4 mm banana connectors that will attach to the test equipment.

When the PCB was delivered, it was visually inspected before assembling. Some modifications were required to fulfill the clearance criteria, these were made using a rotary multitool to machine away the undesired part of the traces.

No compensation of the attenuators were made during the work of this thesis, since this require more time.

Measurements

Since the relay card will be used in measuring pulses with short rise times, it is of importance to know that it does not distort the signal too much. It is desired to measure the magnitude response in the frequency domain, as well as the test pulse in time domain.

To measure the magnitude response, an S21 measurement was performed using the ZVL network analyzer. A fixture was made to mimic the front panel of the CNA 200 to allow for a representative connection of the relay card. The setup can be seen in Figure 3.9a. This setup proved to be unstable at first, as moving the coaxial wires and the grounding wire greatly affected the results for the higher frequencies. Because of the unstable results early in the measuring process, a modification was made to shorten the ground connection by attaching a braid as close as the attenuator grounds as possible and then grounding it directly to the fixture case, as depicted in Figure 3.9b. All subsequent measurements were performed with this modification.

The signal was measured for each output terminal through each of the attenuators to get the magnitude response for the intended use, Figure 3.10a shows this for the + terminal. To see how well the design suppresses unconnected signals, the magnitude response was also measured when the signal was disconnected completely, i.e. all the relays in the fixture were opened as sFigure 3.10b. In addition to this, the magnitude response was also measured with all but the relays on the current terminal closed, seen in Figure 3.10c, to see if there was any overhearing on the circuit board from the other terminals and the traces after the relays. The results were saved both as an image and as raw data in the form of complex numbers in a CSV file to allow for further analysis and plotting.

A single relay was also measured using the network analyzer to get a perception of its high frequency properties. The setup was made by soldering coaxial cable directly to the relay, with as short connecting wires as possible to prevent any influence on the result from the wires. The setup can be seen in Figure 3.9c.

To measure the test pulses through the attenuators, the switching fixture was connected to the CNA 200 and the pulses were measured on the intended connectors using an oscilloscope, as seen in Figure 3.9d. The results were saved both as an image and as data points in a CVS file, for further analysis.

For comparison, the commercial attenuators were also measured in frequency domain with the ZVL and in time domain using the oscilloscope.

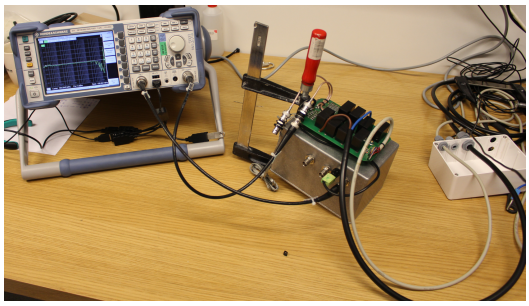

(a) The network analyzer sends its signal into the attenuator through the metallic test rig and receives it back through the BNC outlet of the attenuator.

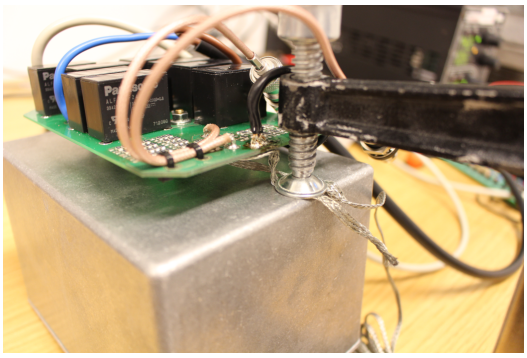

(b) The modified grounding path.

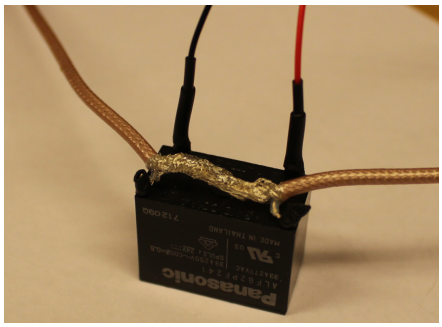

(c) The relay measured with coaxial wires.

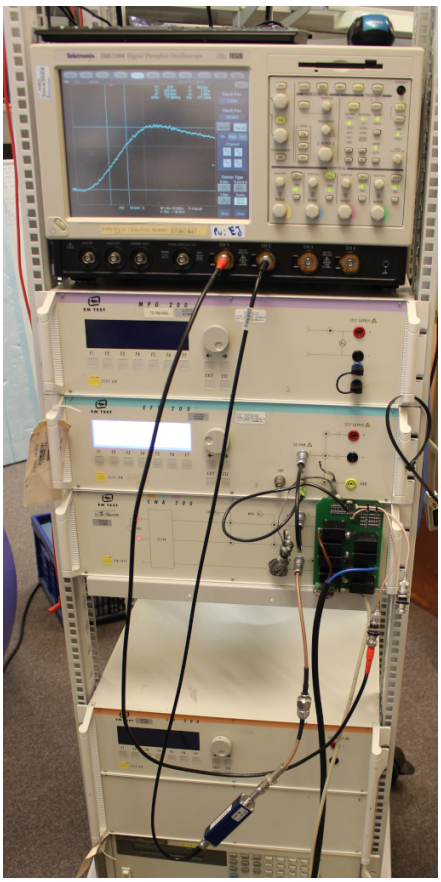

(d) The time measurement setup. Both the commercial and the constructed attenuators were measured in this setup.

Figure 3.9: The test setups for frequency and time measurements of the attenuators.

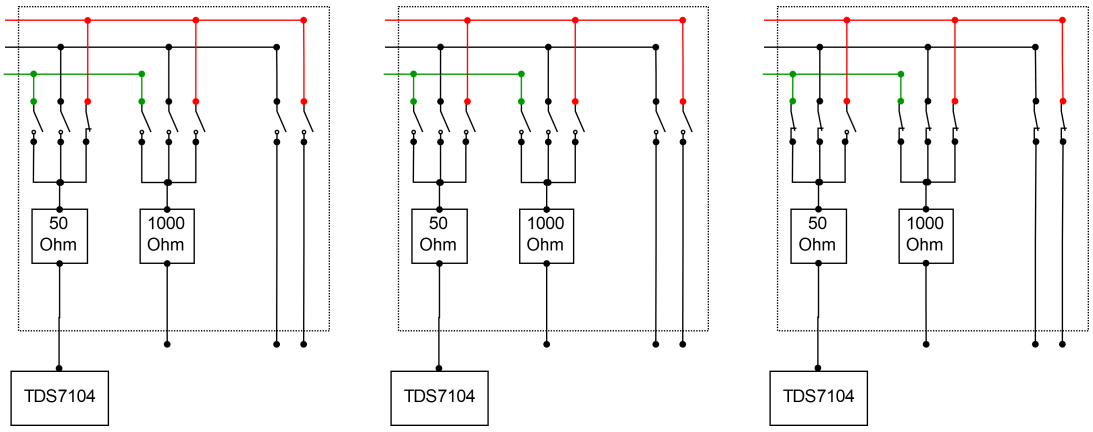

(a) The intended signal through the attenuator.

(b) The isolation of the signal from the cominging terminals to the output of the attenuator.

(c) The isolation of the signal from all other signal paths connected to the output of the attenuator.

Figure 3.10: The different scenarios that were measured in frequency domain for the + terminal to the 50 Ω attenuator. Corresponding measurements were made for the - and the PE terminal as well as for the 1000 Ω attenuator.

4 Results

This chapter presents the results achieved using the methods described in chapter 3. Each section in this chapter corresponds to a section in the method chapter with the same name.

4.1 Prestudy

Since not much was known about the project at this time, it was difficult to find relevant papers on the topic of the standards. Most of the literature was found during the project as new problems was found along the way.

Since the test equipment was mostly in line with the new standards, the first project path was chosen. There was not enough time available to investigate any of the extra tasks as intended.

4.2 Comparison between the old and the new standard

The differences of importance between the old and new standards will be presented in this chapter to see what parameters might be a problem for the older equipment to fulfil.

One of the most notable differences is the removal of a test pulse from ISO 7637-2 that was called *Pulse 5a*. This was instead introduced to the ISO 16750-2 under the name *Load dump A*.

Only the properties that were found to differ are mentioned in the results.

Supply voltages

The specification of the DC supply voltage for the DUT differs in some case between the older and the newer versions of the standard. There are two different supply voltage definitions. U_A represents a system where the generator is in operation and U_B represents the system without the generator in operation. These have different values for 12 V and 24 V systems. U_B is only relevant for Load dump Test A and is thus not defined in ISO 7637 anymore.

Table 4.1 presents the supply voltage specifications from the different standards. The supply voltages are provided by an external PSU and will thus not be dependent on the test equipment.

Table 4.1: Comparison of the different supply voltage specifications.

Standard	Supply voltage U_N =12 V	U_N =24 V
U_A		
ISO 7637-2:2004	13 V to 14 V	26 V to 28 V
ISO 7637-2:2011	12 V to 13 V	24 V to 28 V
ISO 16750-1:2018	13.8 V to 14.2 V	27.8 V to 28.2 V
U_B		
ISO 7637-2:2004	12.3 V to 12.7 V	23.6 V to 24.4 V
ISO 16750-1:2018	12.3 V to 12.7 V	23.8 V to 24.2 V

Surge voltages

Several of the surge voltages has a wider specified range, as can be seen in Table 4.2. Notice how the old pulse 5a and the new load dump A have different specifications for U_S, but they describe the same pulse because of the different definition of U_S in ISO 7637-2 and ISO 16750-2.

Table 4.2: Comparison of the different surge voltage specifications.

Standard	U_S U_N =12 V	U_N =24 V
Pulse 1		
ISO 7637-2:2004	−75 V to −100 V	−450 V to −600 V
ISO 7637-2:2011	−75 V to −150 V	−300 V to −600 V
Pulse 2a		
ISO 7637-2:2004	37 V to 50 V	
ISO 7637-2:2011	37 V to 112 V	
Pulse 3a		
ISO 7637-2:2004	−112 V to −150 V	−150 V to −200 V
ISO 7637-2:2011	−112 V to −220 V	−150 V to −300 V
Pulse 3b		
ISO 7637-2:2004	75 V to 100 V	150 V to 200 V
ISO 7637-2:2011	75 V to 150 V	150 V to 300 V
Pulse 5a/Load dump A		
ISO 7637-2:2004	65 V to 87 V	123 V to 174 V
ISO 16750-2:2012	79 V to 101 V	151 V to 202 V
ISO 16750-2:2012 [1]	65 V to 87 V	123 V to 174 V

Time constraints

The only time constraint that is stricter in the newer standard is the risetime of pulse 3a and pulse 3b, t_r, as shown in Table 4.3

Table 4.3: Comparison of the different time constraints.

Standard	Timing t_d
ISO 7637-2:2004	100 µs to 200 µs
ISO 7637-2:2011	105 µs to 195 µs

[1] Recalculated values to fit the same U_S definitions as the older standard. $U_{S_{7637}} = U_{S_{16750}} - U_{N_{16750}}$

Limits in verification

Most of the limits are the same in all standards. The only differences found are presented in Table 4.4. The tolerances for pulse 1 has been widened to 20 %. The nominal voltage for pulse 2a has been changed to 75 V for calibration but the tolerance is still 10 % with no load.

Table 4.4: Comparison of the limits for calibration.

Pulse 1, U_S, 24 V, 50 Ω load	
ISO 7637-2:2004	−300 V ± 30 V
ISO 7637-2:2011	−300 V ± 60 V
Pulse 2a, U_S, no load	
ISO 7637-2:2004	50 V ± 5 V
ISO 7637-2:2011	75 V ± 7.5 V
Pulse 2a, U_S, 2 Ω load	
ISO 7637-2:2004	25 V ± 5 V
ISO 7637-2:2011	37.5 V ± 7.5 V

4.3 Examination and initial measurement of the old equipment

At first, the test equipment itself needed some care before it was possible to operate it. A couple of screws were loose inside of the LD 200 and a bridge had to be made for the optional external resistor on the MPG 200 for the pulses to even reach the pulse output connectors.

The result from the initial measurements are presented, along with the limits, in Table 4.5 without the CNA 200 connected and in Table 4.6 with the CNA 200 connected.

Table 4.5: The initial manual measurements, measured directly at each generator's output.

	Limits			Measured		
Pulse	U_S (V)	t_d (s)	t_r (s)	U_S (V)	t_d (s)	t_r (s)
Pulse 1, 12 V, Open	[−110, −90]	[1.6, 2.4] m	[0.5, 1] µ	−99.0	2.10 m	540 n
Pulse 1, 24 V, Open	[−660, −540]	[0.8, 1.2] m	[1.5, 3] µ	−630	1.18 m	2.6 µ
Pulse 2a, Open	[67.5, 82.5]	[40, 60] µ	[0.5, 1] µ	76.0	51.0 µ	750 n
Pulse 3a, Open (1k)	[−220, −180]	[105, 195] n	[3.5, 6.5] n	−202	163 n	5.2 n
Pulse 3a, Match	[−120, −80]	[105, 195] n	[3.5, 6.5] n	−104	134 n	5.0 n
Pulse 3b, Open (1k)	[180, 220]	[105, 195] n	[3.5, 6.5] n	202	208 n	5.1 n
Pulse 3b, Match	[80, 120]	[105, 195] n	[3.5, 6.5] n	102	166 n	5.0 n
Load dump A, 12 V, Open	[90, 110]	[320, 480] m	[5, 10] m	93.4	390 m	5.8 m
Load dump A, 24 V, Open	[180, 220]	[280, 420] m	[5, 10] m	190	365 m	5.2 m

Table 4.6: The initial manual measurements on the equipment, including the CNA 200.

	Limits			Measured		
Pulse	U_S (V)	t_d (s)	t_r (s)	U_S (V)	t_d (s)	t_r (s)
Pulse 1, 12 V, Open	[−110, −90]	[1.6, 2.4] m	[0.5, 1] µ	−99.2	2.00 m	450 n
Pulse 1, 24 V, Open	[−660, −540]	[0.8, 1.2] m	[1.5, 3] µ	−632	1.18 m	2.6 µ
Pulse 2a, Open	[67.5, 82.5]	[40, 60] µ	[0.5, 1] µ	76.0	50.0 µ	770 n
Pulse 3a, Open (1k)	[−220, −180]	[105, 195] n	[3.5, 6.5] n	−213	163 n	6.2 n
Pulse 3a, Match	[−120, −80]	[105, 195] n	[3.5, 6.5] n	−93.2	138 n	6.0 n
Pulse 3b, Open (1k)	[180, 220]	[105, 195] n	[3.5, 6.5] n	222	200 n	6.3 n
Pulse 3b, Match	[80, 120]	[105, 195] n	[3.5, 6.5] n	94.0	171 n	5.7 n
Load dump A, 12 V, Open	[90, 110]	[320, 480] m	[5, 10] m	93.2	394 m	5.8 m
Load dump A, 24 V, Open	[180, 220]	[280, 420] m	[5, 10] m	186	400 m	5.1 m

4.4 Test architecture

The 3rd alternative was chosen because of the convenience of a fully automatic system and because of the electrical safety hazard that alternative 2 would pose due to its live measurement connectors.

4.5 Design of dummy loads

The design of the dummy loads is described in this chapter.

Components

The results of the maximum momentary power is shown in Table 4.7. The MPG 200 can generate much higher voltage than the LD 200 which yields a higher momentary power to the dummy loads with these values.

Table 4.7: Calculated momentary worst cases for each dummy load. The LD 200 is included for comparison to the MPG 200 even though it does not result in the highest power.

Dummy load	Generator	R_S	Generator voltage	Resistor peak voltage	Peak resistor power
2 Ω	LD 200	0.5 Ω	200 V	160 V	12.8 kW
2 Ω	MPG 200	2 Ω	600 V	300 V	45 kW
10 Ω	MPG 200	2 Ω	600 V	500 V	5 kW
50 Ω	MPG 200	2 Ω	600 V	577 V	266 W

The maximum energy transferred to the 2 Ω, however, is delivered by the LD 200 generator as shown in Figure 4.1.

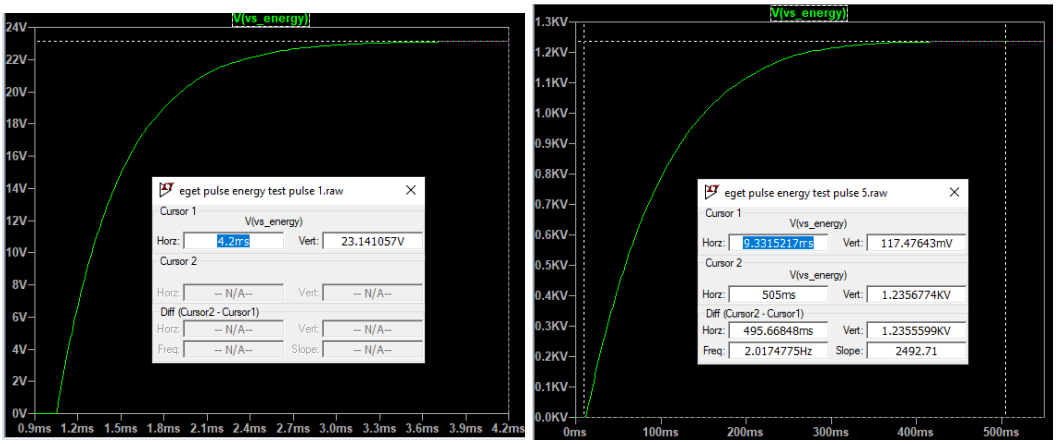

(a) The MPG 200 transfers approximately 23 J to the dummy load.

(b) The LD 200 transfers approximately 1.2 kJ to the dummy load.

Figure 4.1: The maximum energies transferred from the pulse generators to the 2 Ω dummy load. The vertical scale represents the energy in Joule, but is presented in voltage because of the way it is calculated in the simulation.

The LTO100 family[1] from Vishay was chosen because of its high power characteristics and because the maximum overload energy curve was specified in its datasheet. Whith the datasheet and simulation side by side, a worst ratio between the simulated energy and the energy specified in the datasheet was determined. The worst case found for the different pulses and dummy loads can be found in Table 4.8.

[1] `https://www.vishay.com/docs/50051/lto100.pdf`

Table 4.8: The worst case ratio between the simulation energies and the datasheet specification. The ratio equals the minimum number of resistors needed to share the energy.

Dummy load	Ratio	Limiting property
2 Ω	26	Pulse 5 energy after 50 ms
10 Ω	10	Pulse 5 energy after 100 ms
50 Ω	2	Pulse 5 energy after 50 ms

When the least number of resistors required had been determined, some different resistor topologies were considered before setteling on the configuration seen in Figure 4.2. The number of different resistor values was keept as low as considered possible to keep things easy.

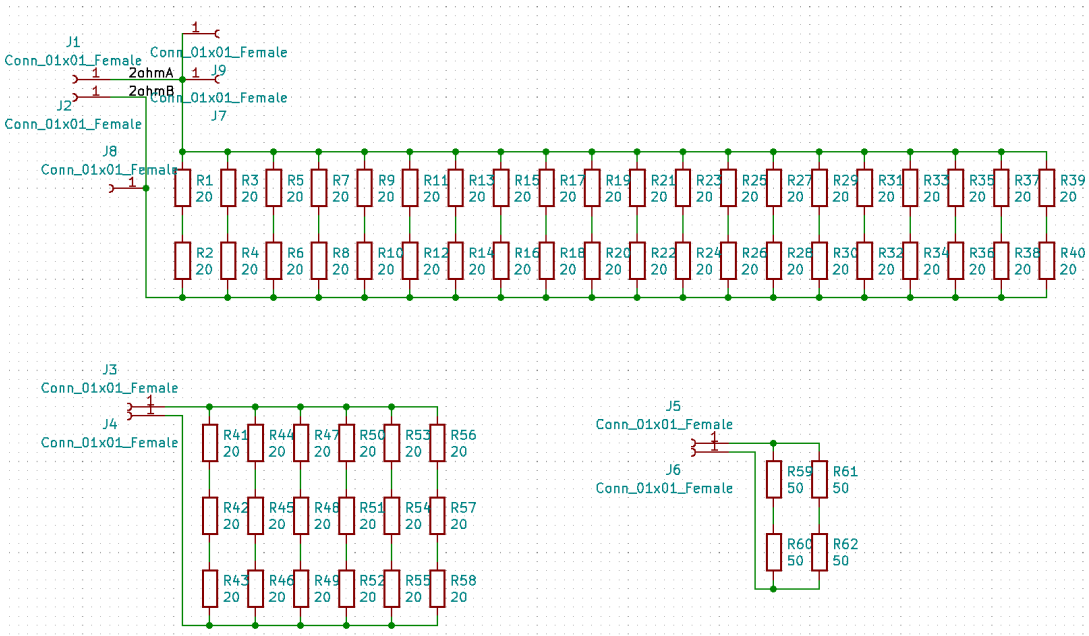

Figure 4.2: The topology chosen for the 2 Ω, 10 Ω and 50 Ω dummy loads.

PCB

Because of the high voltages present on the board, a minumum creepage of 3mm was used. This is in line with the EN 60664-1 standard [4]. The board was perforated to allow for better air flow past the resistors, improving the cooling. The mounting holes for the card was placed in a 105 × 105 mm square, allowing a 120 mm fan to be mounted on top of the card using mounting hardware.

A two layer board was chosen, and all of the traces were mirrored on both layers to get as much conductive cross sectional area as possible, and thus lowering the resistance and power dissipation in the traces. The default copper thickness from the manufacturer[1], was 18 µm, but this PCB was ordered with 60 µm thick copper layer to further extend the cross sectional areas. The width of the traces for the 2 Ω load was chosen as wide as possible without violating the 3 mm creepage distance.

[1] Cogra Pro AB `https://www.cogra.se/produkter/monsterkort/`

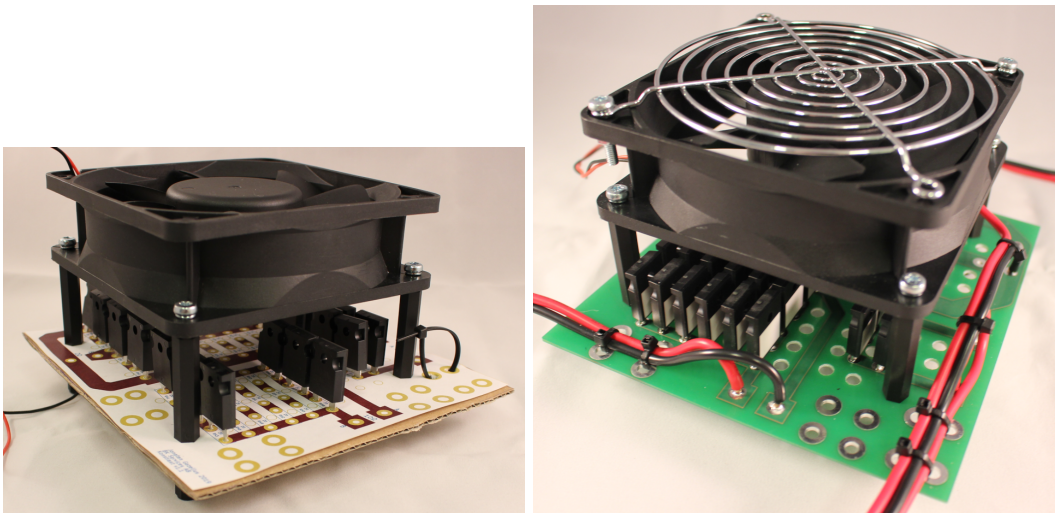

(a) Card board was used to test the PCB layout before it was sent for manufacturing.

(b) The assembled dummy load.

Figure 4.3: The resulting board was predicted using a card board mockup PCB.

When the PCB was delivered, it was visually inspected before assembling. The component placement was correct, but some modification was made to improve the isolation distance by drilling away the plating and pads of the ventilation holes. The modified board's top and bottom side can be seen in Figure 4.4a and Figure 4.4b respectively.

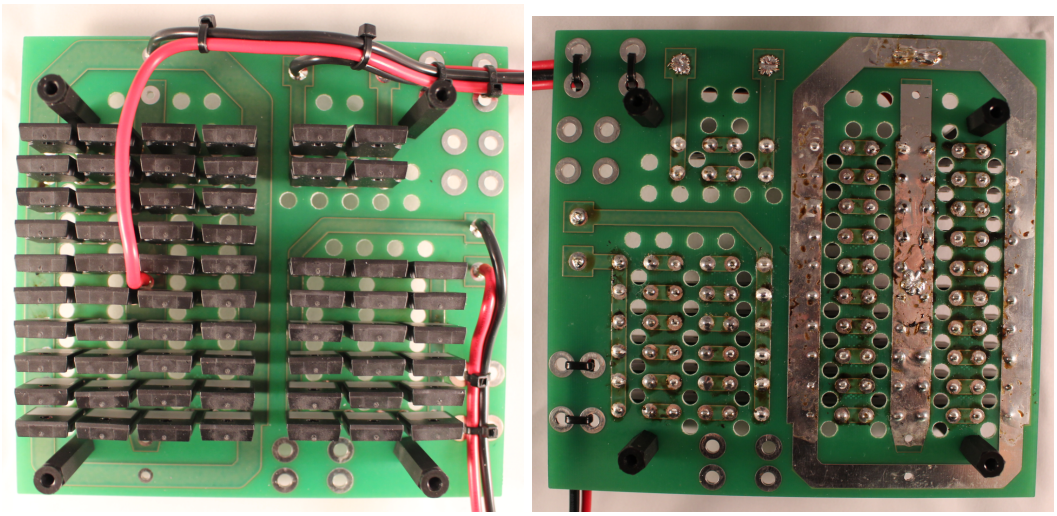

(a) Top.

(b) Bottom.

Figure 4.4: The plating in the ventilation holes was removed by hand using a drill.

Measurements

The resistance of the dummy loads are presented in Table 4.9.

4.6 Design of the switching fixture and the embedded attenuators

The design of the switching fixture and its attenuators is described in this chapter.

Table 4.9: The measured resistance of the dummy loads, and the error compared to the nominal values.

Nominal (Ω)	Measured R (Ω)	Error (%)
2	2.004	+0.2
10	9.973	−0.27
50	49.954	−0.09

Components

The 1206 package from Vishay's CRCW-HP series[1] was used for the embedded attenuators. They are high pulse tolerant thick-film resistors. However, they don't specify the maximum energy vs time as the LTO100 that were used for the dummy loads, but only power and voltage limits. The maximum voltage allowed for the short duration of Pulse 3, 200 ns, is specified to 700 V and the maximum power to 900 W.

The maximum power dissipated into the 50 Ω attenuator will be approximately $\frac{750\,\mathrm{V}^2}{50\,\Omega}$ = 11 250 W. For the 1000 Ω attenuator it will be approximately $\frac{1429\,\mathrm{V}^2}{1000\,\Omega} \approx 2042\,\mathrm{W}$, where 1429 V is the approximate voltage that would result over a 1000 Ω load from a 1500 V source with 50 Ω series resistance.

The Panasonic's LF-G relays were chosen as switching elements as they have a high break-down voltage between the open contacts and had a small form factor making them suitable for the relay box.

Attenuators

The 54.7 dB attenuator was divided into two 27.35 dB Π attenuator links. The values obtained from the online calculator was 54.48 Ω as the parallel resistors and 581.62 Ω as the series resistor. Then the closest values for the resistors was chosen to 54.67 Ω as parallel resistors and 560 Ω as series resistors. The final attenuation was 53.76 dB for the two links according to the simulation, as seen in Figure 4.5a. The design was realized as seen in Figure 4.5c, based on the maximum voltages and powers. Capacitors were placed in the schematic to allow for phase compensation.

Since the uncompensated circuit had its 3 dB limit at only 190 MHz, as seen in Figure 4.5b, the circuit had to be compensated. The results after the compensation can be seen in Figure 4.5d where the new 3 dB limit is instead at 1.7 GHz. The values used for compensating the circuit was 130 pF for the first parallel resistance and 10 pF for the second parallel link as seen in Figure 4.5c.

The 60.1 dB attenuator was divided into one 27.35 dB Π attenuator link, the same as used in the 54.7 dB attenuator, preceded by a 32.75 dB Π link with 1000 Ω in-impedance. When the closest values for the resistors had been chosen, using 56 Ω as parallel resistors and 56 Ω as series resistor, the final attenuation was 60.33 dB for the two links according to the simulation, seen in Figure 4.6a. The attenuator was then realized as seen in Figure 4.6c, based on the maximum voltages and powers.

Since the uncompensated circuit had its 3 dB limit at only 130 MHz, as seen in Figure 4.6b, the circuit had to be compensated. The results after the compensation can be seen in Figure 4.6d where the new 3 dB limit is instead at 2.2 GHz. The values used for compensating the circuit was 40 pF for the first parallel resistance and 30 pF for the second parallel link as seen in Figure 4.6c.

[1] `https://datasheet.octopart.com/CRCW120682R0FKEAHP-Vishay-datasheet-8359436.pdf`

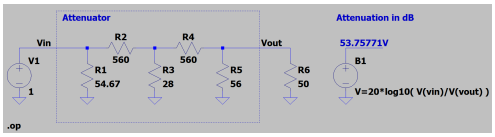

(a) The ideal circuit simulated.

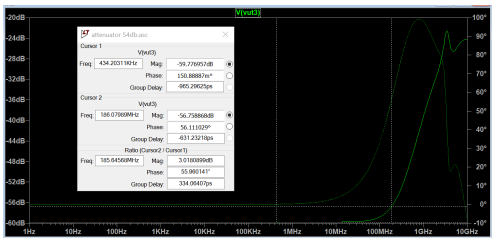

(b) Frequency responce of the circuit with parasitics without compensation.

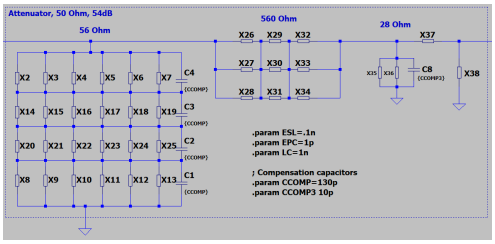

(c) Chosen topology simulated with parasitics and compensation capacitors. The components with designator X are the non-ideal resistors depicted in Figure 2.7

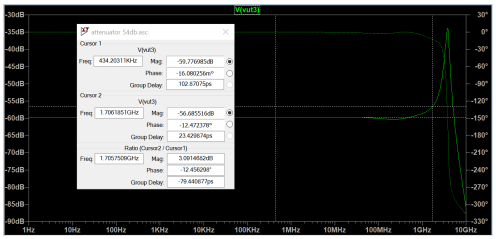

(d) Frequency responce of the circuit with parasitics with compensation capacitors.

Figure 4.5: The 50 Ω attenuator simulated.

PCB

The prototype and finished PCB can be seen side by side in Figure 4.7. The PCB had to be modified after it was delivered, since the creepage distance was to low in a few points and because the footprint for the relays was wrong. The modified PCB can be seen in Figure 4.8.

The manufacturer's default values for dual layer boards was used for this PCB, i.e. 18 µm copper layers on a 1.6 mm laminate.

To attach the relay card fixture to the 4 mm banana connectors on the CNA 200, three banana plugs was designed to be screwed directly to the PCB. This makes the conductors as short as possible, and also act as mechanical fastening of the PCB to the case.

Measurements

The results of the magnitude response measurements can be seen for the 50 Ω attenuator in Figure 4.9 and for the 1 kΩ attenuator in Figure 4.10. The PAT 50 and PAT 1000 attenuators were measured as reference and their results can be seen in Figure 4.11a and Figure 4.12d respectively. The frequency response of the single relay is shown in Figure 4.11c. The footprints for the compensation capacitors has not been populated and the attenuators are thus measured in the uncompensated state.

The time measurements are shown in Figure 4.12

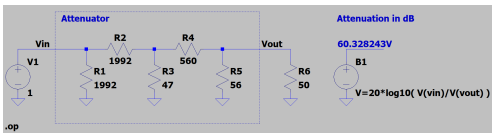

(a) The ideal circuit simulated.

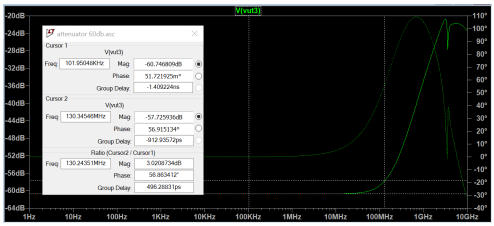

(b) Frequency responce of the circuit with parasitics without compensation.

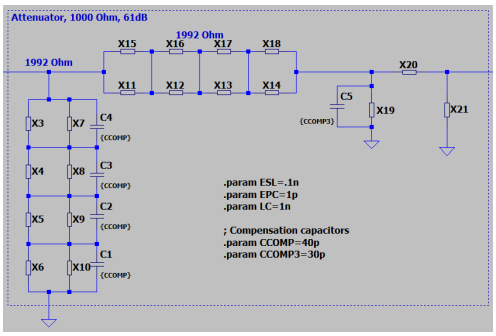

(c) Chosen topology simulated with parasitics and compensation capacitors. The components with designator X are the non-ideal resistors depicted in Figure 2.7

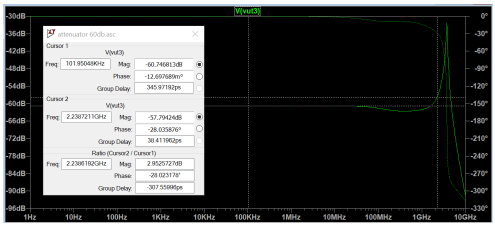

(d) Frequency responce of the circuit with parasitics with compensation capacitors.

Figure 4.6: The 1000 Ω attenuator simulated.

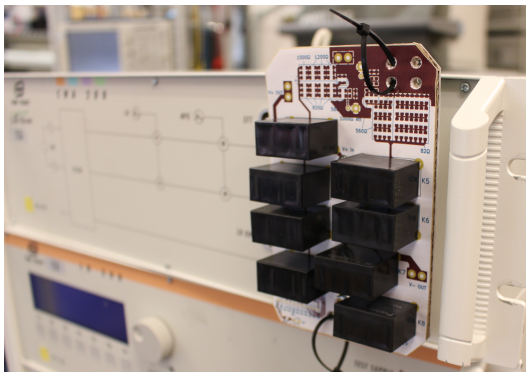

(a) Card board was used to test the PCB layout before it was sent for manufacturing.

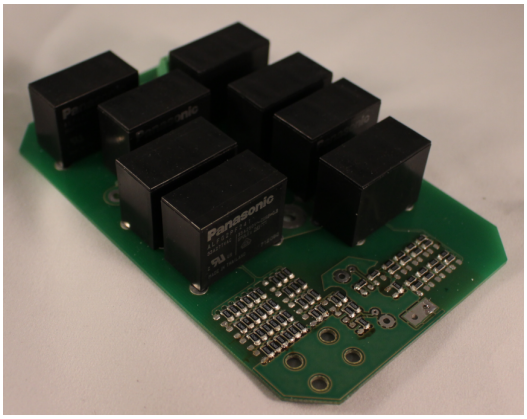

(b) The assembled switching fixture.

Figure 4.7: The resulting board was predicted using a card board mockup PCB.

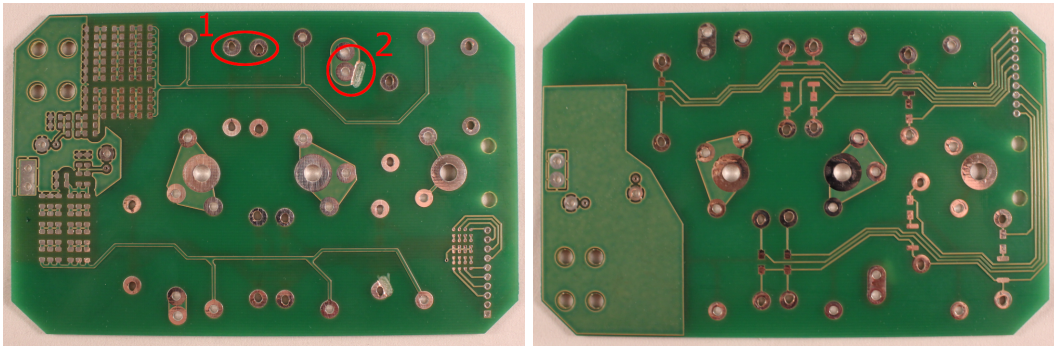

(a) Top. (b) Bottom.

Figure 4.8: The PCB was modified to correct the mistakes. The footprint for the relay was slightly wrong (1) and some of the creepage distances were to short (2)

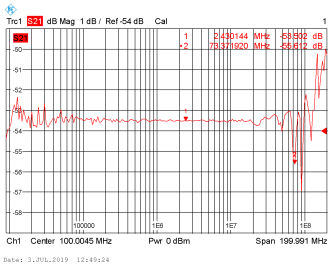

(a) Plus terminal closed, all other open

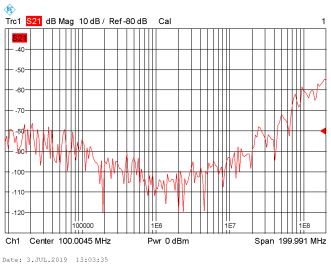

(b) Plus terminal open, all other open

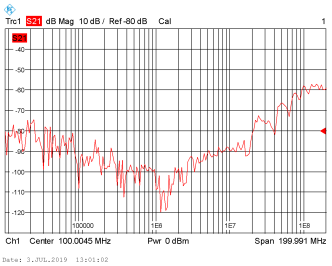

(c) Plus terminal open, all other closed

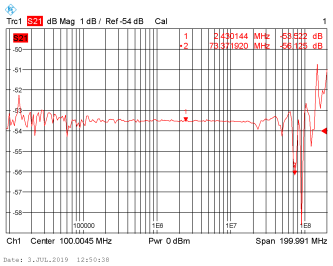

(d) Minus terminal closed, all other open

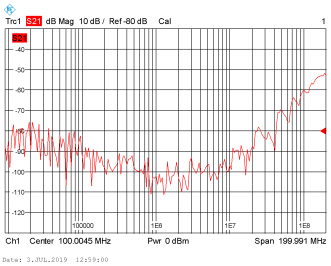

(e) Minus terminal open, all other open

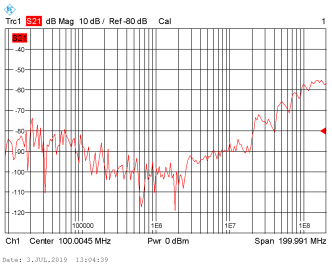

(f) Minus terminal open, all other closed

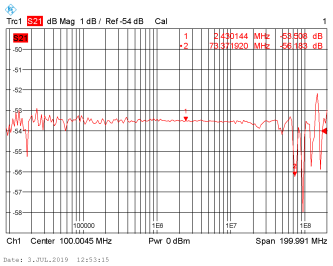

(g) Ground terminal closed, all other open

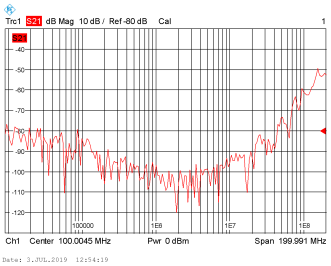

(h) Ground terminal open, all other open

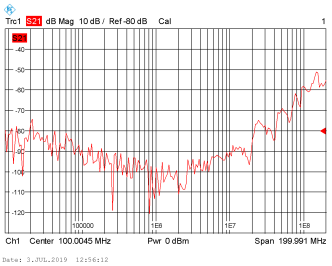

(i) Ground terminal open, all other closed

Figure 4.9: The S21 measurements for the 50 Ω attenuators. No compensation capacitors have been used.

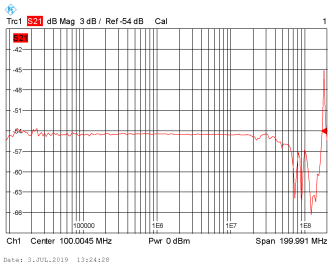

(a) Plus terminal closed, all other open

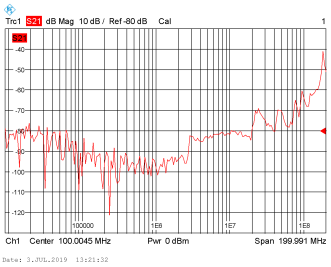

(b) Plus terminal open, all other open

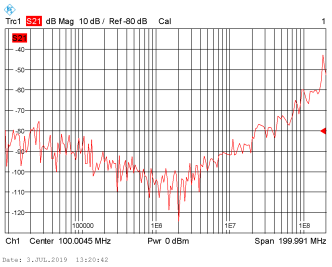

(c) Plus terminal open, all other closed

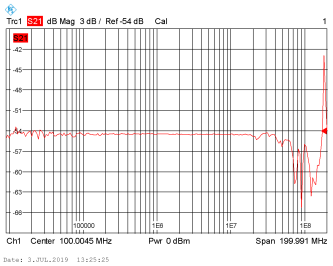

(d) Minus terminal closed, all other open

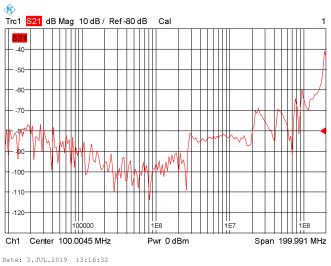

(e) Minus terminal open, all other open

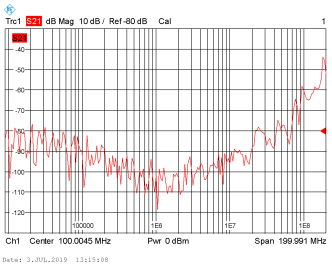

(f) Minus terminal open, all other closed

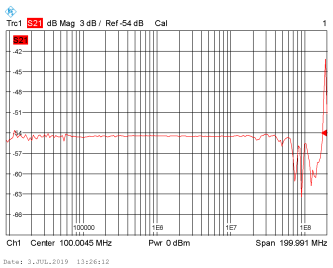

(g) Ground terminal closed, all other open

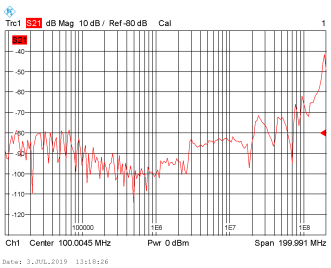

(h) Ground terminal open, all other open

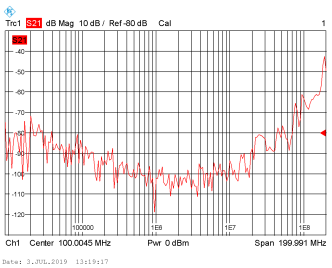

(i) Ground terminal open, all other closed

Figure 4.10: The S21 measurements for the 1 kΩ attenuators. No compensation capacitors have been used.

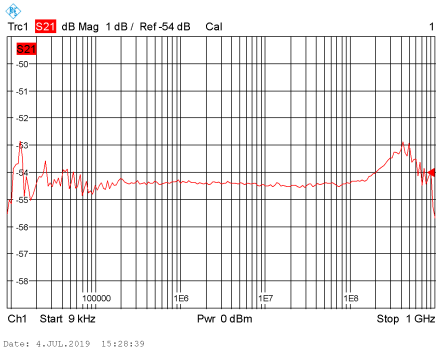

(a) PAT 50

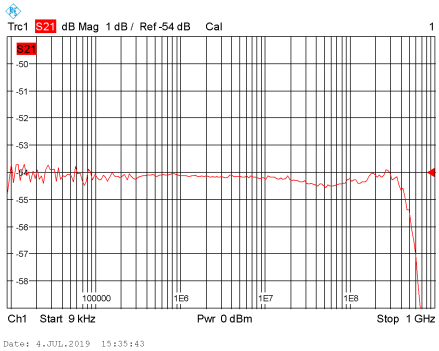

(b) PAT 1000

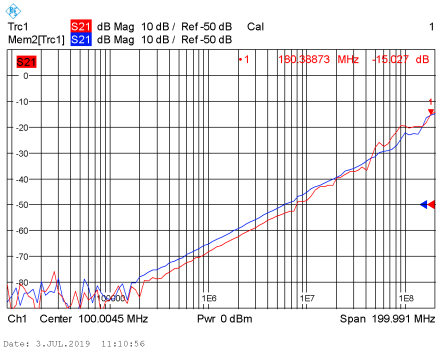

(c) The relay's magnitude response.

Figure 4.11: The S21 measurements on the commercial attenuators and the solo relay.

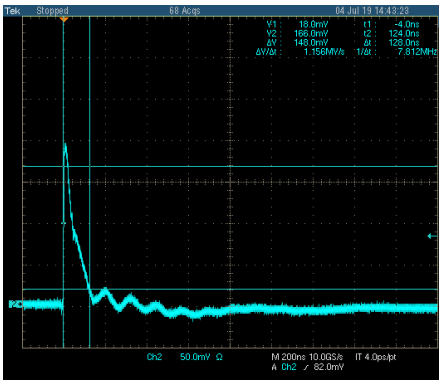

(a) The constructed 50 Ω attenuator

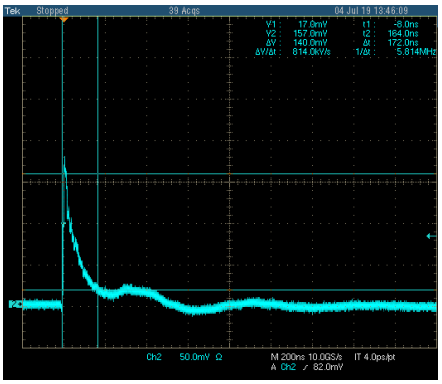

(b) The constructed 1 kΩ attenuator

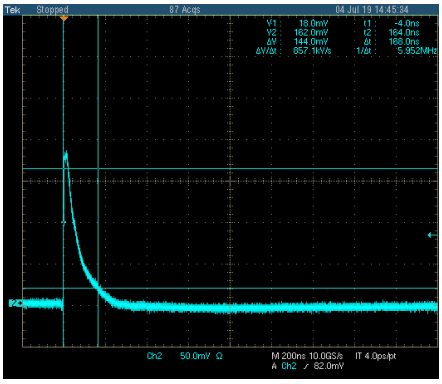

(c) PAT50

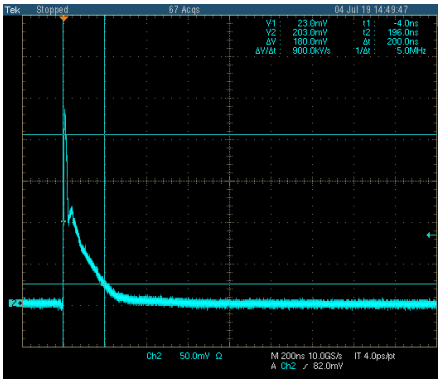

(d) PAT1000

Figure 4.12: The attenuator measurements in time domain, measured with the oscilloscope.

5 Discussion

In this chapter the results and methods are discussed. Source criticism and possible ethical aspects are also brought up.

5.1 Results

The results that need some further explenations and reflections are presented here.

Comparison between the old and the new standard

The old and the new standards proved to be very similar. This was not entirely unexpected, but it helps the future work to have the differences compiled in one place.

Examination and initial measurement of the old equipment

As can be seen in Table 4.5 and Table 4.6, some values exceeded the limits (marked in red). Three of these values even exceeds the old standard's limits, thus indicating that the equipment should probably be usable with the new standard after some service or calibration. With this in mind, the course of the project was targeted towards the design of an automated verification system. With such a verification equipment at hand, the calibration of the generators might be easier to perform as well.

Test architecture

The chosen architecture, with the embedded attenuators, proved to be difficult to implement because of the high frequency design involved. In the future, it might be better to develop a more manual procedure using off the shelf attenuators and a check list. It might be possible to automate the analysis of the results even if the connection of the verification equipment must be made automatically.

Design of dummy loads

The results are well within the 1 % specified by the standard [11]. During tests with the assembled dummy load it seems to work and does not become warm, which indicates that the number of resistors is good or even excessive.

Design of the switching fixture and the embedded attenuators

The attenuators were not populated with compensation capacitors. The results are, in the attenuators current state, not feasible for usage in calibrating the equipment. The required bandwidth for the attenuators must be 400 MHz or greater. The simulated results indicated that this would be the case and that the attenuators will need compensation. But since the actual parasitics in the PCB traces and the design in whole is difficult to know beforehand, the capacitors were left out to start with.

The measured results were pretty unstable and difficult to correlate to the simulated results. Therefore, it is improbable that the compensation capacitors used in the simulation would help in the real world case, at least not with the simulated values. There was no time left in the project to experiment with this.

5.2 Method

The methods that need further explanation and reflections are presented here.

Components

It was surprisingly difficult to find and choose the appropriate components for the dummy load. The resistors had to tolerate extreme surges and the relays had to have high insulation voltages between the contacts. Even finding the encapsulation for the relay box proved to be a challenge, since the filtering options available in the retailer's web stores were not always consistent.

The usage of the energy curve in the datasheet might have been wrong. In this work, the total accumulated energy from time $t = 0$ was considered, but a more reasonable approach would be to test all starting points to find the most extreme energy curve.

Design of attenuators

During the project, the attenuation was considered as the voltage attenuation $att = 20 \times log_{10}\left(\frac{V_{in}}{V_{out}}\right)$ dB. However, the online calculator used was using power attenuation $att = 10 \times log_{10}\left(\frac{P_{in}}{P_{out}}\right)$ dB. The two different ways of expressing attenuation will give the same result if the input impedance is equal to the output impedance. The derived expression seen in Equation 5.1. So to use the online calulator for the 1000 Ω attenuator one would have to specify that you want $60.1\,\text{dB} + 10 \times log_{10}\left(\frac{50}{1000}\right) \approx 47.1\,\text{dB}$. However, this was not known at the time and the values were tweaked manually in LTSpice until the desired attenuation was achieved, but the output impedance was not considered during the tweaking and thereby ended up being a bit mismatched for the next Π link.

$$\begin{aligned} Power\ attenuation &= 10 \times log_{10}\left(\frac{P_{in}}{P_{out}}\right) = 10 \times log_{10}\left(\frac{\frac{U_{in}^2}{R_{in}}}{\frac{U_{out}^2}{R_{out}}}\right) = \\ &= 10 \times log_{10}\left(\left(\frac{U_{in}}{U_{out}}\right)^2 \times \frac{R_{out}}{R_{in}}\right) = 20 \times log_{10}\left(\frac{U_{in}}{U_{out}}\right) + 10 \times log_{10}\left(\frac{R_{out}}{R_{in}}\right) \end{aligned} \tag{5.1}$$

There are infinitely many constellations to approximate the nominal value, in this project it was tried to use as few resistors as possible. This process was performed manually, since no suitable software for solving the problem was found. Thus the chosen constellations might not be optimal.

5.3 Source criticism

Many of the sources are standards from ISO or information from their website. This information can be considered trustworthy since they are the authors of the standards.

The technical note from AVX is based on their own practical experiments, but has no references to any other work. There is a possibility that the methods used were inappropriate or that the results are wrong. They are, however, a manufacturer of capacitors and thus it should be in their interest to have accurate information. The only information used from this, is one of the parasitic values of the resistors, so even if the values are wrong the impact can not be very big.

The same reasoning can be made for the technical note from Vishay. Since they are a manufacturer of resistors they should have accurate information.

The book *High-speed digital design* seems to be widely used.

The book *The circuit designer's companion* doesn't seem to be as widely used, but it is the third edition and can hopefully be considered mostly correct after two revisions.

5.4 The work in a wider context

Test equipment and methodologies can be a very sensitive topic. When a company wants to put a product on the market, they will need to bring their product to a test lab to conduct these tests according to the relevant standards. If the test procedure is wrong, or leaves too much space for interpretations, it could lead to a product failing the test even though it should have passed if the test was made in another lab. Or even worse, an unsafe product might be put on the market due to being falsely passed in the tests. There is always a chance for errors, but using well designed automated systems for testing and verification mitigates the human errors which are the most unpredictable.

6 Conclusion

The main goal of this thesis was to examine the potential of reusing old test equipment with newer standards and how to assure that the results are reliable. A method to verify the test equipment according to the latest standard was suggested in this thesis and some considerations for automating this procedure was made. A dummy load was developed and good enough to be used for verification. The verification system was not completed and the high frequency attenuators did not perform well enough to be used in their current form.

6.1 Research questions

The answers to the research questions are here answered based on the results of the project.

1. Can test equipment made for ISO 7637-2:2004, be used for testing compliance against ISO 7637-2:2011, the newer version of the standard?

Yes, based on the results achieved it most probably can. There are not many of the requirements that have been tougher to meet with the new standard compared to the old. The equipment used in this project failed some of the limits, but the properties that failed are also outside of the old standard's limits.

2. If it can; What considerations must be made to allow for automating the test and verification process?

The output from the pulse generators is hazardous for humans to touch and the system must mitigate the risk of electric shock. Some of the pulse generators are capable of delivering high energies which the calibration loads must be able to withstand. Some of the test pulses contain high frequencies that require the verification system to be well designed for this purpose.

3. If it can't; What causes the failure, and what possible fixes can be made to make the equipment usable for the newer standard?

Not applicable.

6.2 Future work

There were many topics involved in this project that could benefit for some deeper research. The most important ones are mentioned here.

Measurement errors

This is not mentioned in this project, other than tolerances, because it seems to be a very complex and delicate topic. Test equipment, and especially verification equipment, should have a proper error calculation.

Mathematical analysis

When the pulses have been measured, they need to be analysed. The limits for the verifications are amplitudes and durations. To extract these parameters, it could be advantageous to regard the pulse as a mathematical function with certain parameters. It was meant to be investigated in this thesis, but there was not enough time.

Automation of the verification procedure

Most of the equipment used is capable of remote control. It requires a lot of time to design, write and test the software needed to perform the verification automatically. During the time of this thesis some initial tests were made to control the equipment using their GPIB interfaces using C# with successful results, but since there was not enough time to develop anything useful it was left out of this thesis.

Bibliography

[1] R.K. Frazier and S. Alles. "Comparison of ISO 7637 Transient Waveforms to Real World Automotive Transient Phenomena." In: *2005 International Symposium on Electromagnetic Compatibility, 2005. EMC 2005.* 3 (2005), pp. 949–954. DOI: 10.1109/ISEMC.2005.1513662.

[2] ISO. *About us*. [Visited 2019-06-18]. June 2019. URL: https://www.iso.org/about-us.html.

[3] ISO. *Developing standards*. [Visited 2019-06-18]. June 2019. URL: https://www.iso.org/developing-standards.html.

[4] ISO. *EN 60664-1 - Insulation coordination for equipment within low-voltage systems - Part 1: Principles, requirements and tests*. Standard. IEC TC 109, 2007.

[5] ISO. *Guidance on the Systematic Review processing ISO*. Guidance. Available at https://www.iso.org/files/live/sites/isoorg/files/store/en/PUB100413.pdf. Mar. 2019.

[6] ISO. *Shopping FAQs*. [Visited 2019-06-18]. June 2019. URL: https://www.iso.org/shopping-faqs.html.

[7] ISO. *Who develops standards*. [Visited 2019-06-18]. June 2019. URL: https://www.iso.org/who-develops-standards.html.

[8] ISO. *Road vehicles – Environmental conditions and testing for electrical and electronic equipment – Part 1: General*. Standard. ISO/TC 22/SC 32, Nov. 2018.

[9] ISO. *Road vehicles – Environmental conditions and testing for electrical and electronic equipment – Part 2: Electrical loads*. Standard. ISO/TC 22/SC 32, Nov. 2012.

[10] ISO. *Road vehicles – Electrical disturbances from conduction and coupling – Part 1: Definitions and general considerations*. Standard. ISO/TC 22/SC 32, Oct. 2015.

[11] ISO. *Road vehicles – Electrical disturbances from conduction and coupling – Part 2: Electrical transient conduction along supply lines only*. Standard. ISO/TC 22/SC 32, Mar. 2011.

[12] ISO. *Road vehicles – Electrical disturbances from conduction and coupling – Part 3: Electrical transient transmission by capacitive and inductive coupling via lines other than supply lines*. Standard. ISO/TC 22/SC 32, July 2016.

[13] ISO. *Road vehicles – Electrical disturbances from conduction and coupling – Part 5: Enhanced definitions and verification methods for harmonization of pulse generators according to ISO 7637*. Standard. ISO/TC 22/SC 32, Nov. 2016.

[14] AVX Jeffrey Cain. *PARASITIC INDUCTANCE OFMULTILAYER CERAMIC CAPACITORS*. Technical note. Available at `https://www.avx.com/docs/techinfo/CeramicCapacitors/parasitc.pdf`.

[15] Howard Johnson and Martin Graham. *High-speed digital design, a handbook of black magic*. First. Prentice Hall PTR, 1993. ISBN: 0-13-395724-1.

[16] INC. VISHAY INTERTECHNOLOGY. *Frequency Response of Thin Film Chip Resistors*. Technical note. Available at `https://www.vishay.com/docs/60107/freqresp.pdf`. Feb. 2009.

[17] Peter Wilson. *The circuit designer's companion*. Third. Newnes, 2012. ISBN: 978-0-08-097138-4.